

Joint Beam and Channel Tracking for Two-dimensional Phased Antenna Arrays

Yu Liu*, Jiahui Li*, Yin Sun[§], Shidong Zhou*

*Dept. of EE, Tsinghua University, Beijing, 100084, China

[§]Dept. of ECE, Auburn University, Auburn AL, 36849, U.S.A

Abstract—Millimeter wave (mmWave) is an attractive candidate for high-speed mobile communications in the future. However, due to the propagation characteristics of mmWave, beam and alignment becomes a key challenge for serving users with fast moving speeds. In this paper, we develop a joint beam and channel tracking algorithm that can track beams from the horizontal and vertical directions by using two-dimensional (2D) phased antenna arrays. A general sequence of optimal trial beamforming parameters is obtained to achieve the minimum Cramér-Rao lower bound (CRLB) of joint beam and channel tracking asymptotically as antenna number grows to infinity. This sequence is proved to be asymptotically optimal in different conditions, e.g., channel coefficients, path directions, and antenna array sizes. We prove that the proposed algorithm converges to the minimum CRLB in static scenarios. Simulation results show that our algorithm outperforms several existing algorithms in tracking accuracy and speed band.

I. INTRODUCTION

Due to the broad bandwidth of millimeter-wave, the mmWave communication has been considered as one of the key enabling technologies for supporting future wireless applications with extremely high data rate [1]–[3]. However, in mmWave band, only one line-of-sight (LOS) path and a few reflection paths exist as a result of the weak scattering effect [3], [4]. Therefore, beamforming is necessary to make full use of these paths to provide large array gains.

To reduce energy consumption and the hardware cost of radio frequency (RF) chains, analog beamforming with phased antenna arrays is an attractive option [3], [5]–[8]. However, with analog beamforming, one RF chain is connected to multiple antenna elements through reconfigurable phase shifters. Hence only one trial beamforming vector can be applied at each time. As a result, only one observation of the channel from a certain compound antenna pattern is available. Therefore, a sequence of observations from different compound antenna patterns formed by different trial beamforming vectors will be necessary to obtain the channel parameters needed for mmWave transceiver, especially the directions of paths with sufficient strength. Such operations are time-consuming, and may also need sufficient pilots, especially in time-varying channels.

To obtain the needed path directions for analog beamforming, some beam estimation algorithms have been proposed. In [9], [10], beam sweeping is conducted, which sweeps the channel with several spatial beams and estimates the beam directions of the channel according to these observations.

However, these algorithms are based on instantaneous measurements and are suitable for static or quasi-static scenarios. The estimation accuracy degrades when the pilot overhead is limited in time-varying channels. In order to obtain higher accuracy, prior information of beam directions needs to be taken into account. Hence, beam tracking methods are introduced, where the estimated beam direction is updated based on prior observations and estimations [11]–[14]. However, the trial beamforming vectors are not optimized in those tracking algorithms, resulting in a waste of transmission energy.

A beam tracking algorithm is proposed in [15], [16], trying to optimize the sequence of trial beamforming vectors, assuming the channel coefficient is known. In [17], the authors start to jointly track channel coefficient and beam direction with optimal trial beamforming vectors. However, these algorithms are based on linear antenna arrays, which can only support one-dimensional (1D) beam tracking. While in several mobile scenarios, e.g., dense urban area [18] and unmanned aerial vehicle (UAV) scenarios [19], the beam may also come from different horizontal and vertical directions. Hence, we need to dynamically track the 2D beam direction with 2D phased antenna arrays.

This problem is challenging due to the following three reasons: (i) with analog beamforming, we can only obtain part of the system information through one observation. (ii) We need to jointly track channel coefficient and 2D beam direction and the trial beamforming vectors need to be dynamically adjusted. Therefore, it is a dynamic joint optimization problem with a sequential trial beamforming vectors and these trial beamforming vectors also need to be optimized. (iii) Compared with 1D beam direction, more trial beamforming vectors are required when tracking 2D beam direction. As a result, the optimization dimension greatly increases.

In this paper, we aim to develop a beam and channel tracking algorithm to handle the problem above, the main contributions and results are summarized as follows:

- We prove that at least three different trial directions are needed to jointly track the channel coefficient and 2D beam directions.
- In static scenarios, the Cramér-Rao lower bound (CRLB) of beam and channel tracking with 2D phased antenna arrays is obtained, which is a function of the trial beamforming vectors. We optimize these trial beamforming vectors and get the minimum CRLB. A general way to generate the trial beamforming vectors is proposed with a

set of parameters which are proved to be asymptotically optimal in different conditions, e.g., channel coefficients, path directions and antenna arrays.

- We design a joint beam and channel tracking algorithm for 2D phased antenna arrays. In addition, we prove that this algorithm can converge to the minimum CRLB with high probability in static scenarios.
- Simulation results show that our algorithm approaches the minimum CRLB quickly in static scenarios. In dynamic scenarios, our algorithm can achieve lower tracking error and faster tracking speed compared with several existing algorithms.

II. SYSTEM MODEL

We consider the planar phased antenna array receiver¹. To estimate and track the beam direction at the receiver end, q fixed pilot symbols s_p are sent from the transmitter in each time-slot k , where $|s_p|^2 = E_p$ is the transmit power of each pilot symbol. As described above, only a few paths exist in mmWave channel. Because the angle spread is small and the mmWave system can be configured with a large number of antennas, the interaction between multi-paths is relatively weak, making it possible to track each path independently [20]. Hence, we focus on the method for tracking one path and different paths can be tracked separately by using the same method.

Consider the planar antenna array receiver in Fig. 1, where $M \times N$ antennas are placed in a rectangular area, with a distance d_1 (d_2) between neighboring antennas along x -axis (y -axis)². All the antennas are connected to the same RF chain through different phase shifters. In time-slot k , the incident beam of the considered path arrives at the planar antennas from an elevation angle of arrival (AoA) $\theta_k \in [0, \pi/2)$ and azimuth AoA $\varphi_k \in [-\pi, \pi)$. Hence, the channel vector of the considered path is given by

$$\mathbf{h}_k = \beta_k \mathbf{a}(\mathbf{x}_k), \quad (1)$$

where $\beta_k = \beta_k^{\text{re}} + j\beta_k^{\text{im}}$ is the complex channel coefficient, $\mathbf{x}_k = [x_{k,1}, x_{k,2}]^T = \left[\frac{Md_1 \cos(\theta_k) \cos(\varphi_k)}{\lambda}, \frac{Nd_2 \cos(\theta_k) \sin(\varphi_k)}{\lambda} \right]^T$ is the normalized beam direction,

$$\mathbf{a}(\mathbf{x}_k) = [a_{11}(\mathbf{x}_k) \cdots a_{1N}(\mathbf{x}_k) \ a_{21}(\mathbf{x}_k) \cdots a_{MN}(\mathbf{x}_k)]^T \quad (2)$$

is the steering vector with $a_{mn}(\mathbf{x}_k) = e^{j2\pi(\frac{m-1}{M}x_{k,1} + \frac{n-1}{N}x_{k,2})}$ ($m = 1, \dots, M; n = 1, \dots, N$), and λ is the wavelength.

Let $\mathbf{w}_{k,i}$ be the trial beamforming vector for receiving the i -th ($i = 1, \dots, q$) pilot symbol in time-slot k . In this paper, we use $\mathbf{w}_{k,i}$ in the form of steering vector to ensure sufficient array gain, given by

¹Note that tracking is needed at both the transmitter and receiver. However, considering the transmitter-receiver reciprocity, the beam and channel tracking of both sides will have similar designs. Hence, we focus on beam and channel tracking algorithm design and performance analysis on the receiver side.

²To obtain different resolutions in horizontal direction and vertical direction, the antenna numbers along different directions may not be the same, i.e., $M \neq N$ [21]. To suppress sidelobe, the antennas may be unequally spaced, i.e., $d_1 \neq d_2$ [22].

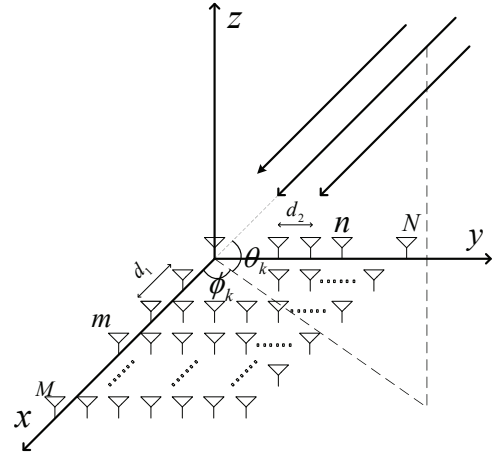


Fig. 1. 2D phased antenna array.

$$\mathbf{w}_{k,i} = \frac{1}{\sqrt{MN}} \mathbf{a}(\boldsymbol{\Gamma}_{k,i}), \quad (3)$$

where $\boldsymbol{\Gamma}_{k,i}$ is the trial beam direction. After phase shifting and combining, the observation at the baseband output of RF chain is given by

$$y_{k,i} = \mathbf{w}_{k,i}^H \mathbf{h}(\mathbf{x}_k) s_p + z_{k,i} = s_p \beta_k \mathbf{w}_{k,i}^H \mathbf{a}(\mathbf{x}_k) + z_{k,i}, \quad (4)$$

where $z_{k,i} \sim \mathcal{CN}(0, \sigma^2)$ is an *i.i.d.* circularly symmetric complex Gaussian random variable. Define $\boldsymbol{\Psi}_k \triangleq [\beta_k^{\text{re}}, \beta_k^{\text{im}}, x_{k,1}, x_{k,2}]^T$ as the channel parameter vector in time-slot k , trial beamforming matrix $\mathbf{W}_k \triangleq [\mathbf{w}_{k,1}, \mathbf{w}_{k,2}, \dots, \mathbf{w}_{k,q}]$, and the noise vector $\mathbf{z}_k \triangleq [z_{k,1}, z_{k,2}, \dots, z_{k,q}]$. Then the conditional probability density function of the observation vector $\mathbf{y}_k \triangleq [y_{k,1}, y_{k,2}, \dots, y_{k,q}]^T$ is given by

$$p(\mathbf{y}_k | \boldsymbol{\Psi}_k, \mathbf{W}_k) = \frac{1}{\pi^q \sigma^2 q} e^{-\frac{\|\mathbf{y}_k - s_p \beta_k \mathbf{W}_k^H \mathbf{a}(\mathbf{x}_k)\|_2^2}{\sigma^2}}. \quad (5)$$

In time-slot k , the receiver needs to choose a trial beamforming matrix \mathbf{W}_k and obtain an estimate $\hat{\boldsymbol{\Psi}}_k \triangleq [\hat{\beta}_k^{\text{re}}, \hat{\beta}_k^{\text{im}}, \hat{x}_{k,1}, \hat{x}_{k,2}]$ of the channel coefficient β_k and normalized beam direction \mathbf{x}_k . From a control system perspective, $\boldsymbol{\Psi}_k$ is the system state, $\hat{\boldsymbol{\Psi}}_k$ is the estimate of the system state, the trial beamforming matrix \mathbf{W}_k is the control action and \mathbf{y}_k is the noisy observation.

III. PROBLEM FORMULATION AND OPTIMIZATION OF TRIAL BEAMFORMING MATRIX

Let $\zeta = (\mathbf{W}_1, \mathbf{W}_2, \dots, \hat{\boldsymbol{\Psi}}_1, \hat{\boldsymbol{\Psi}}_2, \dots)$ denote a beam and channel tracking scheme. We consider a particular set Ξ of *causal* beam tracking policies: based on the previously used trial beamforming matrix $\mathbf{W}_1, \mathbf{W}_2, \dots, \mathbf{W}_{k-1}$ and historical observations $\mathbf{y}_1, \mathbf{y}_2, \dots, \mathbf{y}_{k-1}$, choose an appropriate trial beamforming matrix \mathbf{W}_k , apply it to get \mathbf{y}_k and make an estimation of channel parameters in time-slot k .

A. Problem Formulation

In k -th time-slot, the beam and channel tracking problem is formulated as:

$$\min_{\zeta \in \Xi} \frac{1}{MN} \mathbb{E} \left[\left\| \hat{\mathbf{h}}_k - \mathbf{h}_k \right\|_2^2 \right] \quad (6)$$

$$\text{s.t. } \mathbb{E} [\hat{\mathbf{h}}_k] = \mathbf{h}_k, \quad (7)$$

where the constraint (7) makes sure that $\hat{\mathbf{h}}_k \triangleq \hat{\beta}_k \mathbf{a}(\hat{\mathbf{x}}_k)$ is an unbiased estimation of the channel vector $\mathbf{h}_k = \beta_k \mathbf{a}(\mathbf{x}_k)$.

Problem (6) is hard to solve optimally due to the following reasons: (i) we can only obtain part of the system information through observation \mathbf{y}_k . (ii) The trial beamforming matrix \mathbf{W}_k and the estimate $\hat{\Psi}_k$ need to be optimized. However, both the optimization of control action \mathbf{W}_k and the optimization of estimate $\hat{\Psi}_k$ are non-convex problems.

Before giving some theoretical results of problem (6), we will first study the pilot overhead of beam and channel tracking with 2D phased antenna arrays.

B. How Many Pilots Are Needed for Estimation?

For linear antenna arrays, at least two pilots are required in each time-slot [17]. When tracking the channel coefficient and 2D beam directions with 2D phased antenna arrays, four pilots ($q = 4$) are feasible, where each of the two dimensions can be tracked by using two pilots. However, we should achieve tracking with as few pilots as possible since the pilot resource is so precious. As illustrated in (4), one complex observation corresponds to two real number equations. Then the following lemma is introduced to help determine the smallest q :

Lemma 1. *If the trial beamforming vectors are in the steering vector form, then only $q+1$ independent real number equations are obtained by q observations in time-slot k .*

Proof. See Appendix A in [23]. ■

Lemma 1 tells us how many independent real number equations are obtained by using q observations. According to Lemma 1, at least three observations are required in each time-slot to obtain four independent real number equations and estimate four real variables. Hence, the smallest pilot number in each time-slot is $q = 3$, i.e., the trial beamforming matrix $\mathbf{W}_k = [\mathbf{w}_{k,1}, \mathbf{w}_{k,2}, \mathbf{w}_{k,3}]$.

C. Lower Bound of Tracking Error

The huge challenge to solve problem (6) optimally makes it hard to complete in just one paper. Therefore, we make a few simplifications and perform some theoretical analysis for static scenarios as the first step in this paper.

Consider the problem of tracking a static beam, where $\Psi_k = \Psi \triangleq [\beta^{\text{re}}, \beta^{\text{im}}, x_1, x_2]^T$ for all time-slots. Since the channel vector $\hat{\mathbf{h}}_k$ is not linear with respect to Ψ , the CRLB of channel vector mean square error (MSE) cannot be given directly by the traditional unbiased estimation theory in [24]. To handle this, we introduce the following lemma:

Lemma 2. *The MSE of channel vector in (6) is lower bounded as follows:*

$$\begin{aligned} & \frac{1}{MN} \mathbb{E} \left[\left\| \hat{\mathbf{h}}_k - \mathbf{h}_k \right\|_2^2 \right] \\ & \geq \frac{1}{MN} \text{Tr} \left\{ \left(\sum_{l=1}^k \mathbf{I}(\Psi, \mathbf{W}_l) \right)^{-1} \sum_{m=1}^M \sum_{n=1}^N (\mathbf{v}_{m,n}^H \mathbf{v}_{m,n}) \right\}, \end{aligned} \quad (8)$$

where $\mathbf{v}_{m,n} \triangleq [1, j, j2\pi \frac{m-1}{M} \beta, j2\pi \frac{n-1}{N} \beta]$ and the Fisher

information matrix $\mathbf{I}(\Psi, \mathbf{W}_k)$ is given by

$$\begin{aligned} \mathbf{I}(\Psi, \mathbf{W}_k) & \triangleq -\mathbb{E} \left[\frac{\partial \log p(\mathbf{y}_k | \Psi, \mathbf{W}_k)}{\partial \Psi} \cdot \frac{\partial \log p(\mathbf{y}_k | \Psi, \mathbf{W}_k)}{\partial \Psi^T} \right] \\ & = \frac{2|s_p|^2}{\sigma^2} \begin{bmatrix} \|\mathbf{g}_k\|_2^2 & 0 & \text{Re}\{\mathbf{g}_k^H \tilde{\mathbf{g}}_{k1}\} & \text{Re}\{\mathbf{g}_k^H \tilde{\mathbf{g}}_{k2}\} \\ 0 & \|\tilde{\mathbf{g}}_{k1}\|_2^2 & \text{Im}\{\mathbf{g}_k^H \tilde{\mathbf{g}}_{k1}\} & \text{Im}\{\mathbf{g}_k^H \tilde{\mathbf{g}}_{k2}\} \\ \text{Re}\{\mathbf{g}_k^H \tilde{\mathbf{g}}_{k1}\} & \text{Im}\{\mathbf{g}_k^H \tilde{\mathbf{g}}_{k1}\} & \|\tilde{\mathbf{g}}_{k1}\|_2^2 & \text{Re}\{\tilde{\mathbf{g}}_{k1}^H \tilde{\mathbf{g}}_{k2}\} \\ \text{Re}\{\mathbf{g}_k^H \tilde{\mathbf{g}}_{k2}\} & \text{Im}\{\mathbf{g}_k^H \tilde{\mathbf{g}}_{k2}\} & \text{Re}\{\tilde{\mathbf{g}}_{k1}^H \tilde{\mathbf{g}}_{k2}\} & \|\tilde{\mathbf{g}}_{k2}\|_2^2 \end{bmatrix}, \end{aligned}$$

with $\mathbf{g}_k = \mathbf{W}_k^H \mathbf{a}(\mathbf{x})$, $\tilde{\mathbf{g}}_{k1} = \beta \mathbf{W}_k^H \frac{\partial \mathbf{a}(\mathbf{x})}{\partial x_1}$, and $\tilde{\mathbf{g}}_{k2} = \beta \mathbf{W}_k^H \frac{\partial \mathbf{a}(\mathbf{x})}{\partial x_2}$.

Proof. See Appendix B in [23]. ■

Lemma 2 tells us the CRLB of the channel vector MSE, which is a function of the trial beamforming matrices $\mathbf{W}_1, \dots, \mathbf{W}_k$. Optimizing these trial beamforming matrices, we can get the minimum CRLB. Therefore, the performance bound of (6) can be formulated as

$$\begin{aligned} \text{MSE}_{\text{opt}} & = \min_{\mathbf{W}_1, \dots, \mathbf{W}_k} \frac{1}{MN} \text{Tr} \left\{ \left(\sum_{l=1}^k \mathbf{I}(\Psi, \mathbf{W}_l) \right)^{-1} \sum_{m=1}^M \sum_{n=1}^N (\mathbf{v}_{m,n}^H \mathbf{v}_{m,n}) \right\} \\ & \stackrel{(a)}{=} \min_{\mathbf{W}} \frac{1}{MN} \text{Tr} \left\{ (k \mathbf{I}(\Psi, \mathbf{W}))^{-1} \sum_{m=1}^M \sum_{n=1}^N (\mathbf{v}_{m,n}^H \mathbf{v}_{m,n}) \right\} \\ & \stackrel{(b)}{=} \min_{\mathbf{W}} u(\Psi, \mathbf{W}), \end{aligned} \quad (10)$$

where Step (a) is due to the linear additivity of the Fisher information matrix [25] and Step (b) is due to the definition of $u(\Psi, \mathbf{W})$:

$$u(\Psi, \mathbf{W}) \triangleq \frac{1}{MN} \text{Tr} \left\{ (k \mathbf{I}(\Psi, \mathbf{W}))^{-1} \sum_{m=1}^M \sum_{n=1}^N (\mathbf{v}_{m,n}^H \mathbf{v}_{m,n}) \right\}, \quad (11)$$

which is a function of the trial beamforming matrix \mathbf{W} and holds for any q . Hence, we can optimize just one trial beamforming matrix \mathbf{W} and let $\mathbf{W}_1^* = \mathbf{W}_2^* = \dots = \mathbf{W}_k^* = \mathbf{W}^*$ to obtain the minimum CRLB by (10).

D. Asymptotically Optimal Trial Beamforming Matrix

Let us consider the optimal trial beamforming matrix \mathbf{W}^* . We first rewrite the trial beamforming vectors in (3) as

$$\mathbf{w}_{k,i} = \frac{1}{\sqrt{MN}} \mathbf{a}(\mathbf{x} + \Delta_{k,i}), \quad i = 1, 2, 3, \quad (12)$$

where $\Delta_{k,i} = [\delta_{k,i1}, \delta_{k,i2}]^T$ denotes the i -th trial beam direction offset in time-slot k . $\Delta_{k,i}$ has two features:

1) According to [17], $\Delta_{k,i}$ should be within the main lobe set $\mathcal{B}(\mathbf{x})$ of the normalized direction \mathbf{x} , i.e.,

$$\mathcal{B}(\mathbf{x}) \triangleq (x_1 - 1, x_1 + 1) \times (x_2 - 1, x_2 + 1). \quad (13)$$

2) By (10), the optimal trial beam direction offsets are fixed with $\Delta_{k,i}^* = \Delta_i^* = [\delta_{i,1}^*, \delta_{i,2}^*]^T$ in different time-slots since $\mathbf{W}_1^* = \mathbf{W}_2^* = \dots = \mathbf{W}_k^* = \mathbf{W}^*$.

With these two features above, we try to find Δ_i^* to obtain the optimal trial beamforming matrix \mathbf{W}^* .

For 1D linear antenna arrays, the optimal two trial beam direction offsets are obtained by using numerical method [17]. For 2D phased antenna arrays, three 2D trial beam direction offsets need to be optimized and can not be obtained directly via [17]. It is hard to get analytical results for such a six-dimensional non-convex problem. Numerical search is a feasible way to handle the problem. However, $\Delta_1^*, \Delta_2^*, \Delta_3^*$ may

TABLE I
ASYMPTOTICALLY OPTIMAL TRIAL BEAM DIRECTION OFFSETS.

$\tilde{\delta}_{1,1}^*$	$\tilde{\delta}_{1,2}^*$	$\tilde{\delta}_{2,1}^*$	$\tilde{\delta}_{2,2}^*$	$\tilde{\delta}_{3,1}^*$	$\tilde{\delta}_{3,2}^*$
0.0963	0.5098	-0.5098	-0.0963	0.2906	-0.2906

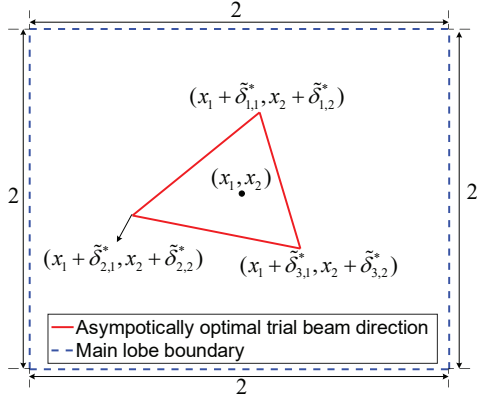


Fig. 2. Asymptotically optimal trial beam direction offsets.

be related to some system parameters, e.g., channel coefficient β , normalized beam direction \mathbf{x} and antenna array size M, N . Once these system parameters change, numerical search has to be re-conducted, leading to high complexity. Fortunately, the good features of the optimal trial beam direction offsets $\Delta_1^*, \Delta_2^*, \Delta_3^*$ can help us overcome the challenge:

Lemma 3. *If the trial beamforming vectors are in the steering vector form and the optimal trial beam direction offsets are denoted as $\Delta_1^*, \Delta_2^*, \Delta_3^*$, then:*

- 1) $\Delta_1^*, \Delta_2^*, \Delta_3^*$ are unrelated to channel coefficient β ;
- 2) $\Delta_1^*, \Delta_2^*, \Delta_3^*$ are irrelevant to the normalized beam direction \mathbf{x} ;
- 3) $\Delta_1^*, \Delta_2^*, \Delta_3^*$ converge to constant values as $M, N \rightarrow +\infty$:

$$\tilde{\Delta}_i^* \triangleq \lim_{M, N \rightarrow +\infty} \Delta_i^*, i = 1, 2, 3.$$

Proof. See Appendix C in [23].

Lemma 3 reveals that $\Delta_1^*, \Delta_2^*, \Delta_3^*$ are only related to array size M, N . Hence, the numerical search complexity can be reduced to one for a particular array size M, N . Even if $\Delta_1^*, \Delta_2^*, \Delta_3^*$ may change for different array sizes, we can adopt $\tilde{\Delta}_1^*, \tilde{\Delta}_2^*, \tilde{\Delta}_3^*$ to take the place of $\Delta_1^*, \Delta_2^*, \Delta_3^*$ as long as M and N are sufficiently large. Therefore, the numerical search times are reduced to one.

The asymptotically optimal trial beam direction offsets $\tilde{\Delta}_1^*, \tilde{\Delta}_2^*, \tilde{\Delta}_3^*$ obtained by numerical search in the main lobe (13) are shown in TABLE I and Fig. 2. Since $\tilde{\Delta}_1^*, \tilde{\Delta}_2^*, \tilde{\Delta}_3^*$ are asymptotically optimal as M, N grow to infinity, how do they work when antenna number is not sufficiently large? We adopt the $\tilde{\Delta}_1^*, \tilde{\Delta}_2^*, \tilde{\Delta}_3^*$ to smaller size antenna arrays and compare the performance of $\tilde{\Delta}_1^*, \tilde{\Delta}_2^*, \tilde{\Delta}_3^*$ and $\Delta_1^*, \Delta_2^*, \Delta_3^*$ as M, N grow. As illustrated in Fig. 3, when antenna number $M = N \geq 8$, we can approach the approximate minimum CRLB with an relative error less than 0.1% by using $\tilde{\Delta}_1^*, \tilde{\Delta}_2^*, \tilde{\Delta}_3^*$. Therefore, with $\tilde{\Delta}_1^*, \tilde{\Delta}_2^*, \tilde{\Delta}_3^*$, the minimum CRLB is obtained

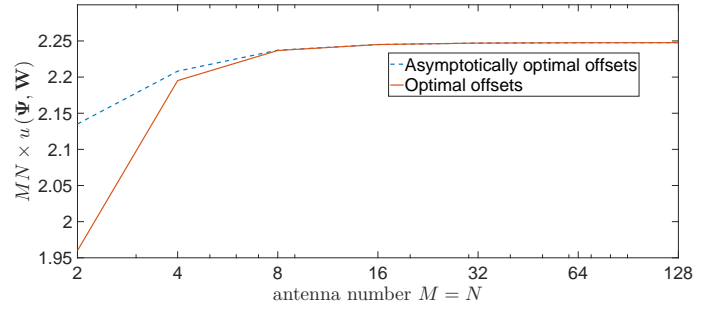


Fig. 3. Performance of asymptotically optimal offsets.

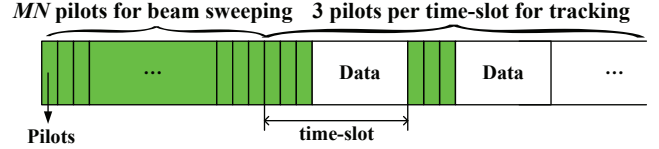


Fig. 4. Frame structure.

for different normalized beam directions, different channel coefficients and different antenna numbers when $M = N \geq 8$.

Hence, a general way to generate the asymptotically optimal trial beamforming matrix $\tilde{\mathbf{W}}_k^* = [\tilde{\mathbf{w}}_{k,1}^*, \tilde{\mathbf{w}}_{k,2}^*, \tilde{\mathbf{w}}_{k,3}^*]$ is obtained to achieve the minimum CRLB as below:

$$\tilde{\mathbf{w}}_{k,i}^* = \frac{1}{\sqrt{MN}} \mathbf{a}(\mathbf{x} + \tilde{\Delta}_i^*), i = 1, 2, 3. \quad (14)$$

IV. JOINT BEAM AND CHANNEL TRACKING WITH ASYMPTOTIC OPTIMALITY ANALYSIS

A. Joint Beam and Channel Tracking

The proposed tracking algorithm is similar to that in [17]. The main difference is that we need $M \times N$ pilots to estimate the initial normalized beam direction and three trial beamforming vectors to track the time-varying normalized beam direction.

Joint Beam and Channel Tracking:

- 1) **Coarse Beam Sweeping:** As shown in Fig. 4, $M \times N$ pilots are received successively. The trial beamforming vector corresponding to the observation $\tilde{\mathbf{y}}_{m,n}$ is $\tilde{\mathbf{w}}_{m,n} = \frac{1}{\sqrt{MN}} \mathbf{a} \left(\left[\frac{(2m-1-M)d_1}{\lambda}, \frac{(2n-1-N)d_2}{\lambda} \right]^T \right)$, $m = 1, \dots, M, n = 1, \dots, N$. The initial estimate of $\hat{\Psi}_0 = [\hat{\beta}_0^{\text{re}}, \hat{\beta}_0^{\text{im}}, \hat{x}_{0,1}, \hat{x}_{0,2}]^T$ is obtained by:

$$\hat{\mathbf{x}}_0 = \underset{\hat{\mathbf{x}} \in \chi}{\text{argmax}} |\mathbf{a}(\hat{\mathbf{x}})^H \tilde{\mathbf{W}} \tilde{\mathbf{y}}|, \quad \hat{\beta}_0 = [\tilde{\mathbf{W}}^H \mathbf{a}(\hat{\mathbf{x}}_0)]^+ \tilde{\mathbf{y}}, \quad (15)$$

where $\chi = \left\{ \left[\frac{(2m-1-M_0)d_1}{\lambda M_0}, \frac{(2n-1-N_0)d_2}{\lambda N_0} \right]^T \mid m=1, \dots, M_0, n=1, \dots, N_0 \right\}$, $M_0 \times N_0$ is the codebook size with $M_0 \geq M$ and $N_0 \geq N$, $\tilde{\mathbf{y}} = [\tilde{y}_{11}, \tilde{y}_{12}, \dots, \tilde{y}_{MN}]^T$, $\tilde{\mathbf{W}} = [\tilde{\mathbf{w}}_{11}, \tilde{\mathbf{w}}_{12}, \dots, \tilde{\mathbf{w}}_{MN}]$, and $\mathbf{X}^+ = (\mathbf{X}^H \mathbf{X})^{-1} \mathbf{X}^H$.

- 2) **Beam and channel tracking:** In time-slot k , three pilots are received by using trial beamforming vectors given below:

$$\mathbf{w}_{k,i} = \frac{1}{\sqrt{MN}} \mathbf{a}(\hat{\mathbf{x}}_{k-1} + \tilde{\Delta}_i^*), i = 1, 2, 3, \quad (16)$$

where $\hat{\mathbf{x}}_k \triangleq [\hat{x}_{k,1}, \hat{x}_{k,2}]$. The estimate $\hat{\Psi}_k = [\hat{\beta}_k^{\text{re}}, \hat{\beta}_k^{\text{im}}, \hat{x}_{k,1}, \hat{x}_{k,2}]$ is updated by

$$\hat{\Psi}_k = \hat{\Psi}_{k-1} + \frac{2}{\sigma^2} b_k \mathbf{I} \left(\hat{\Psi}_{k-1}, \mathbf{W}_k \right)^{-1} \begin{bmatrix} \text{Re} \{ s_p^H \mathbf{e}_k^H (\mathbf{y}_k - \hat{\mathbf{y}}_k) \} \\ \text{Im} \{ s_p^H \mathbf{e}_k^H (\mathbf{y}_k - \hat{\mathbf{y}}_k) \} \\ \text{Re} \{ s_p^H \tilde{\mathbf{e}}_{k1}^H (\mathbf{y}_k - \hat{\mathbf{y}}_k) \} \\ \text{Re} \{ s_p^H \tilde{\mathbf{e}}_{k2}^H (\mathbf{y}_k - \hat{\mathbf{y}}_k) \} \end{bmatrix}, \quad (17)$$

where $\mathbf{e}_k = \mathbf{W}_k^H \mathbf{a}(\hat{\mathbf{x}}_{k-1})$, $\hat{\mathbf{y}}_k = s_p \hat{\beta}_{k-1} \mathbf{W}_k^H \mathbf{a}(\hat{\mathbf{x}}_{k-1})$, $\tilde{\mathbf{e}}_{k1} = \mathbf{W}_k^H \frac{\partial \mathbf{a}(\hat{\mathbf{x}}_{k-1})}{\partial x_1}$ and $\tilde{\mathbf{e}}_{k2} = \mathbf{W}_k^H \frac{\partial \mathbf{a}(\hat{\mathbf{x}}_{k-1})}{\partial x_2}$. Here, b_k is the step size and will be specified later.

B. Asymptotic Optimality Analysis

In the recursive procedure (17), there exist multiple stable points and these stable points correspond to the local optimal points of the beam and channel tracking problem. We first prove that the normalized beam direction and channel coefficient Ψ is a stable point. The main proof method is similar to [17]. The difference is that the vectors here are 4-dimensional. Due to space limitations, the detailed proof is included in [17].

Even if Ψ is a stable point, how can we ensure that the tracking procedure converges to Ψ rather than other local optimal points? To resolve this challenge, we develop the corresponding theorem to study the convergence of our algorithm.

we adopt the diminishing step-size in (18), given by [24], [26], [27]

$$b_k = \frac{\epsilon}{k + K_0}, k = 1, 2, \dots \quad (18)$$

where $K_0 \geq 0$ and $\epsilon > 0$.

Theorem 1 (Convergence to a Unique Stable Point). *If b_k is given by (18) with $\epsilon > 0$ and $K_0 \geq 0$, then $\hat{\Psi}_k$ converges to a unique stable point with probability one.*

Proof. See Appendix D. ■

Therefore, for the general step-size in (18), $\hat{\Psi}_k$ converges to a unique stable point.

Theorem 2 (Convergence to Real Normalized Beam Direction \mathbf{x}). *If (i) $\hat{\mathbf{x}}_0 \in \mathcal{B}(\mathbf{x})$ and (ii) b_k is given by (18) with $\epsilon > 0$, then there exist some $K_0 \geq 0$ and $C > 0$ such that*

$$P(\hat{\mathbf{x}}_k \rightarrow \mathbf{x} \mid \hat{\mathbf{x}}_0 \in \mathcal{B}(\mathbf{x})) = 1 - 8e^{-\frac{C|s_p|^2}{\epsilon^2 \sigma^2}}. \quad (19)$$

Proof. See Appendix E. ■

At the coarse beam sweeping stage of JRBCT algorithm, the initial estimation $\hat{\mathbf{x}}_0$ within main lobe $\mathcal{B}(\mathbf{x})$ in (13) can be obtained with high probability. Under the condition $\hat{\mathbf{x}}_0 \in \mathcal{B}(\mathbf{x})$, Theorem 2 tells us the probability of $\hat{\mathbf{x}}_k \rightarrow \mathbf{x}$ is related to $\frac{|s_p|^2}{\epsilon^2 \sigma^2}$. Hence, we can reduce the step-size and increase the transmit SNR $\frac{|s_p|^2}{\sigma^2}$ to make sure that $\hat{\mathbf{x}}_k \rightarrow \mathbf{x}$ with probability one.

Theorem 3 (Convergence to \mathbf{x} with minimum CRLB). *If (i) $\hat{\Psi}_k \rightarrow \Psi_k$ and (ii) b_k is given by (18) with $\epsilon = 1$ and any $K_0 \geq 0$, then*

$$\lim_{k \rightarrow \infty} k \mathbb{E} \left[\left\| \hat{\beta}_k \mathbf{a}(\hat{\mathbf{x}}_k) - \beta_k \mathbf{a}(\mathbf{x}_k) \right\|_2^2 \right] = \text{MSE}_{\text{opt}}. \quad (20)$$

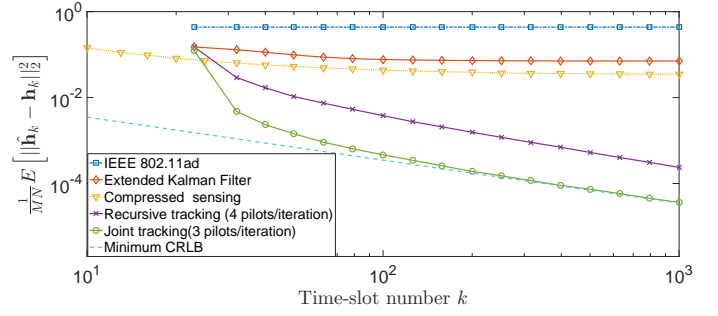


Fig. 5. $\frac{1}{MN} \text{MSE}_{\mathbf{h}_k}$ vs. time-slot number k in static beam tracking.

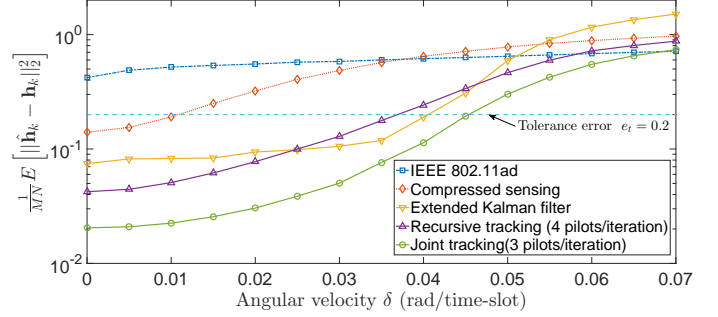


Fig. 6. $\frac{1}{MN} \text{MSE}_{\mathbf{h}_k}$ vs. angular velocity in dynamic beam tracking scenarios.

Proof. See Appendix F. ■

Theorem 3 tells us ϵ should not be too large or too small. By Theorem 3, if $\epsilon = 1$, then we achieve the minimum CRLB asymptotically with high probability.

V. NUMERICAL RESULTS

We compare the proposed algorithm with four other algorithms: the compressed sensing algorithm in [28], the IEEE 802.11ad algorithm in [11], the extended Kalman filter (EKF) method in [14] and the recursive beam and channel tracking algorithm given by [17] (using two pilots to track each dimension of the 2D beam direction). In each time-slot, three pilots are transmitted for all the algorithms to ensure fairness. When adopting the recursive beam and tracking algorithm by using four pilots, we use a buffer to store the received pilots and update the estimate when receiving four new pilots. Based on the model in Section II, the parameters are set as: $M = N = 8$, the antenna spacing $d_1 = d_2 = \frac{\lambda}{2}$, the codebook size $M_0 = 2M$, $N_0 = 2N$, the pilot symbol $s_p = 1$, the channel coefficient $\beta_k = \frac{1+j}{\sqrt{2}}$ and transmit SNR $= \frac{|s_p|^2}{\sigma^2} = 0\text{dB}$.

In static scenarios, the AoA (θ, ϕ) as defined in Section II is chosen evenly and randomly in $\theta \in [0, \frac{\pi}{2}]$, $\phi \in [-\pi, \pi]$. The step-size b_k is set as $b_k = \frac{1}{k}$. Simulation results are averaged over 1000 random system realizations. Fig. 5 indicates that the channel vector MSE of our proposed algorithm approaches the minimum CRLB quickly and achieves much lower tracking error than other algorithms.

In dynamic scenarios, the AoA (θ, ϕ) as defined in Section II is modeled as a random walk process, i.e., $\theta(k+1) = \theta(k) + \Delta\theta$, $\phi(k+1) = \phi(k) + \Delta\phi$; $\Delta\theta, \Delta\phi \sim \mathcal{CN}(0, \sigma^2)$. The initial AoA value is chosen evenly and randomly in $\theta(0) \in [0, \frac{\pi}{2}]$,

$\phi(0) \in [-\pi, \pi)$. As for the step-size b_k , we adopt the constant step-size. Numerical results show that when $b_k = 0.7$, the joint beam and channel tracking algorithm can track beams with higher velocity. Therefore, the step-size is set as a constant $b_k = 0.7$. Fig. 5 indicates the proposed algorithm can achieve higher tracking accuracy than the other four algorithms. In addition, if we set a tolerance error e_t , e.g., $e_t = 0.2$, then our algorithm can support higher angular velocities.

VI. FUTURE WORK REMARKS

In this paper, we have developed a joint beam and channel tracking algorithm for 2D phased antenna array. A general sequence of optimal trial beamforming parameters is obtained to achieve the minimum CRLB. The work is a first step to beam and channel tracking with 2D phased antenna arrays. We perform some theoretical analysis in static scenarios. However, the convergence and optimality of the proposed algorithm in dynamic scenarios are not proven here. Besides, the constant step-size used in dynamic scenarios is not proven to be optimal. We will establish the corresponding theorems in our future work.

Another interesting aspect is tracking in a more realistic mmWave communication system. First of all, we have considered the single-path beam and channel tracking in this paper and will study the joint beam and channel tracking algorithm to track multiple paths simultaneously in our future work. Second, we focus on tracking the AoAs at receiver in this paper. In our future work, we will develop the algorithm that can jointly track the channel coefficient and the beam directions at both the transmitter and receiver.

REFERENCES

- [1] Z. Pi and F. Khan, "An introduction to millimeter-wave mobile broadband systems," *IEEE Commun. Mag.*, vol. 49, no. 6, Jun. 2011.
- [2] F. Boccardi, R. W. Heath, A. Lozano, T. L. Marzetta, and P. Popovski, "Five disruptive technology directions for 5G," *IEEE Commun. Mag.*, vol. 52, no. 2, Feb. 2014.
- [3] R. W. Heath, N. González-Prelcic, S. Rangan, W. Roh, and A. M. Sayeed, "An overview of signal processing techniques for millimeter wave MIMO systems," *IEEE J. Sel. Top. Signal Process.*, Apr. 2016.
- [4] T. S. Rappaport, G. R. MacCartney, M. K. Samimi, and S. Sun, "Wideband millimeter-wave propagation measurements and channel models for future wireless communication system design," *IEEE Trans. Commun.*, vol. 63, no. 9, Sep. 2015.
- [5] S. Sun, T. S. Rappaport, R. W. Heath, A. Nix, and S. Rangan, "MIMO for millimeter-wave wireless communications: Beamforming, spatial multiplexing, or both?" *IEEE Commun. Mag.*, vol. 52, no. 12, Dec. 2014.
- [6] S. Han, C. L. I, Z. Xu, and C. Rowell, "Large-scale antenna systems with hybrid analog and digital beamforming for millimeter wave 5G," *IEEE Commun. Mag.*, vol. 53, no. 1, Jan. 2015.
- [7] A. Puglielli, A. Townley, G. LaCaille, V. Milovanovi, P. Lu, K. Trotskovsky, A. Whitcombe, N. Narevsky, G. Wright, T. Courtade, E. Alon, B. Nikoli, and A. M. Niknejad, "Design of energy- and cost-efficient massive MIMO arrays," *Proc. IEEE*, vol. 104, no. 3, Mar. 2016.
- [8] A. F. Molisch, V. V. Ratnam, S. Han, Z. Li, S. L. H. Nguyen, L. Li, and K. Haneda, "Hybrid beamforming for massive MIMO-a survey," *IEEE Commun. Mag.*, vol. 55, no. 9, Sep. 2017.
- [9] D. Zhu, J. Choi, and R. W. Heath Jr, "Auxiliary beam pair enabled AoD and AoA estimation in closed-loop large-scale mmwave mimo system," *arXiv preprint arXiv:1610.05587*, 2016.
- [10] A. Alkhateeb, G. Leus, and R. W. Heath, "Limited feedback hybrid precoding for multi-user millimeter wave systems," *IEEE Trans. Wireless Commun.*, vol. 14, no. 11, Nov. 2015.
- [11] IEEE standard, "IEEE 802.11ad WLAN enhancements for very high throughput in the 60 GHz band," Dec. 2012.
- [12] J. Palacios, D. De Donno, and J. Widmer, "Tracking mm-Wave channel dynamics: Fast beam training strategies under mobility," *IEEE INFOCOM*, 2017.
- [13] X. Gao, L. Dai, Y. Zhang, T. Xie, X. Dai, and Z. Wang, "Fast channel tracking for Terahertz beamspace massive MIMO systems," *IEEE Trans. Veh. Technol.*, vol. 66, no. 7, Jul. 2017.
- [14] V. Va, H. Vikalo, and R. W. Heath, "Beam tracking for mobile millimeter wave communication systems," in *IEEE GlobalSIP*, Dec. 2016.
- [15] J. Li, Y. Sun, L. Xiao, S. Zhou, and C. E. Koksall, "Fast analog beam tracking in phased antenna arrays: Theory and performance," *arXiv preprint arXiv:1710.07873*, 2017.
- [16] —, "Analog beam tracking in linear antenna arrays: Convergence, optimality, and performance," in *51st Asilomar Conference*, 2017.
- [17] J. Li, Y. Sun, L. Xiao, S. Zhou, and A. Sabharwal, "How to mobilize mmWave: A joint beam and channel tracking approach," *arXiv preprint arXiv:1802.02125*, 2018.
- [18] T. S. Rappaport, F. Gutierrez, E. Ben-Dor, J. N. Murdock, Y. Qiao, and J. I. Tamir, "Broadband millimeter-wave propagation measurements and models using adaptive-beam antennas for outdoor urban cellular communications," *IEEE Trans. Antennas and Propagation*, vol. 61, no. 4, Apr. 2013.
- [19] G. Brown, O. Koymen, and M. Branda, "The promise of 5G mmWave - How do we make it mobile?" *Qualcomm Technologies*, Jun. 2016.
- [20] Z. Xiao, P. Xia, and X. gen Xia, "Enabling uav cellular with millimeter-wave communication: potentials and approaches," *IEEE Commun. Mag.*, vol. 54, no. 5, May. 2016.
- [21] W. Roh, J. Y. Seol, J. Park, B. Lee, J. Lee, Y. Kim, J. Cho, K. Cheun, and F. Aryanfar, "Millimeter-wave beamforming as an enabling technology for 5G cellular communications: Theoretical feasibility and prototype results," *IEEE Commun. Mag.*, vol. 52, no. 2, Feb. 2014.
- [22] R. Bhattacharya, T. K. Bhattacharyya, and R. Garg, "Position mutated hierarchical particle swarm optimization and its application in synthesis of unequally spaced antenna arrays," *IEEE Trans. Antennas and Propagation*, vol. 60, no. 7, Jul. 2012.
- [23] Y. Liu, J. Li, Y. Sun, and S. Zhou, "Joint beam and channel tracking for 2d antenna arrays," *arXiv preprint arXiv:1804.06258*, 2018.
- [24] M. B. Nevel'son and R. Z. Has'minskii, *Stochastic approximation and recursive estimation*, 1973.
- [25] H. V. Poor, *An introduction to signal detection and estimation*. New York, NY, USA: Springer-Verlag New York, Inc., 1994.
- [26] V. S. Borkar, *Stochastic approximation: a dynamical systems viewpoint*, 2008.
- [27] H. Kushner and G. G. Yin, *Stochastic approximation and recursive algorithms and applications*. Springer Science & Business Media, 2003, vol. 35.
- [28] A. Alkhateeb, G. Leus, and R. W. Heath, "Compressed sensing based multi-user millimeter wave systems: How many measurements are needed?" in *IEEE ICASSP*, Apr. 2015.
- [29] S. Sengijpta, "Fundamentals of statistical signal processing: Estimation theory," *Technometrics*, vol. 37, Nov. 1995.

APPENDIX A PROOF OF LEMMA 1

If the phase shifts are steering vectors with $\mathbf{w}_{k,i} = \frac{1}{\sqrt{MN}} \mathbf{a}(\mathbf{x} + \Delta_{k,i})$, where $\Delta_{k,i} = [\delta_{k,i1}, \delta_{k,i2}]^T$ denotes the i -th trial normalized direction offset, then we get the two complex equations (21) (22) ignoring noise for the i -th and j -th ($i \neq j$) observations:

$$y_{k,i} = \frac{s_p \beta}{\sqrt{MN}} \sum_{m=1}^M \sum_{n=1}^N e^{-j2\pi \left(\frac{(m-1)\delta_{k,i1}}{M} + \frac{(n-1)\delta_{k,i2}}{N} \right)} \quad (21)$$

$$y_{k,j} = \frac{s_p \beta}{\sqrt{MN}} \sum_{m=1}^M \sum_{n=1}^N e^{-j2\pi \left(\frac{(m-1)\delta_{k,j1}}{M} + \frac{(n-1)\delta_{k,j2}}{N} \right)} \quad (22)$$

Separating amplitude and phase angle parts of $y_{k,i}$ and $y_{k,j}$, we obtain

$$\alpha(y_{k,i}) = \alpha(s_p \beta) - \pi \left[\frac{M-1}{M} \delta_{k,i1} + \frac{N-1}{N} \delta_{k,i2} \right] \quad (23)$$

$$\alpha(y_{k,j}) = \alpha(s_p \beta) - \pi \left[\frac{M-1}{M} \delta_{k,j1} + \frac{N-1}{N} \delta_{k,j2} \right], \quad (24)$$

where $\alpha(y)$ denotes the phase angle of y .

Combining (23) and (24), we can get the following relationship between the phase angle of $y_{k,i}$ and $y_{k,j}$:

$$\begin{aligned} & \alpha(y_{k,i}) - \alpha(y_{k,j}) \\ &= \pi \left[\frac{M-1}{M} (\delta_{k,j1} - \delta_{k,i1}) + \frac{N-1}{N} (\delta_{k,j2} - \delta_{k,i2}) \right]. \end{aligned} \quad (25)$$

The phase angle of $y_{k,i}$ and $y_{k,j}$ are correlated as (25) reveals since $\delta_{k,i1} - \delta_{k,j1}$ and $\delta_{k,i2} - \delta_{k,j2}$ are determined by trial beam direction and already known before tracking. Thus, we can obtain q independent amplitude equations and only 1 independent phase angle equation after q observations, which are $q+1$ independent real number equations in total.

APPENDIX B PROOF OF LEMMA 2

If $f(\hat{\mathbf{x}})$ is an unbiased estimation of parameter $f(\mathbf{x})$ with $\mathbb{E}[f(\hat{\mathbf{x}})] = f(\mathbf{x})$, then we can obtain

$$\text{Var}[f(\hat{\mathbf{x}})] \geq \frac{\partial f(\mathbf{x})}{\partial \mathbf{x}} \mathbf{I}(\mathbf{x})^{-1} \left(\frac{\partial f(\mathbf{x})}{\partial \mathbf{x}} \right)^H \quad (26)$$

according to [29]. Given $h_{mn}(\Psi) = \beta e^{j2\pi(\frac{m-1}{M}x_1 + \frac{n-1}{N}x_2)}$, we have $\mathbb{E}[h_{mn}(\hat{\Psi})] = h_{mn}(\Psi)$ and the partial derivative of $h_{mn}(\Psi)$ is:

$$\begin{cases} \frac{\partial h_{mn}(\Psi)}{\partial \beta^{re}} = e^{j2\pi(\frac{m-1}{M}x_1 + \frac{n-1}{N}x_2)} \\ \frac{\partial h_{mn}(\Psi)}{\partial \beta^{im}} = j e^{j2\pi(\frac{m-1}{M}x_1 + \frac{n-1}{N}x_2)} \\ \frac{\partial h_{mn}(\Psi)}{\partial x_1} = j 2\pi \frac{m-1}{M} \beta e^{j2\pi(\frac{m-1}{M}x_1 + \frac{n-1}{N}x_2)} \\ \frac{\partial h_{mn}(\Psi)}{\partial x_2} = j 2\pi \frac{n-1}{N} \beta e^{j2\pi(\frac{m-1}{M}x_1 + \frac{n-1}{N}x_2)} \end{cases} \quad (27)$$

Combining (6), (26) and (27), we have

$$\begin{aligned} & \frac{1}{MN} \mathbb{E} \left[\left\| \hat{\mathbf{h}}_k - \mathbf{h}_k \right\|_2^2 \right] \\ &= \frac{1}{MN} \sum_{m=1}^M \sum_{n=1}^N \mathbb{E} \left[|h_{mn}(\hat{\Psi}) - h_{mn}(\Psi)|^2 \right] \\ &\stackrel{(a)}{\geq} \frac{1}{MN} \sum_{m=1}^M \sum_{n=1}^N \left(\mathbf{v}_{mn} \left(\sum_{l=1}^k \mathbf{I}(\Psi, \mathbf{W}_l) \right)^{-1} \mathbf{v}_{mn}^H \right) \\ &= \frac{1}{MN} \text{Tr} \left\{ \left(\sum_{l=1}^k \mathbf{I}(\Psi, \mathbf{W}_l) \right)^{-1} \sum_{m=1}^M \sum_{n=1}^N (\mathbf{v}_{mn}^H \mathbf{v}_{mn}) \right\}, \end{aligned} \quad (28)$$

where step (a) is obtained by substituting (27) into (26).

Hence, Lemma 2 is proved.

APPENDIX C PROOF OF LEMMA 3

Lemma 3 is proved in three steps:

Step 1: We prove that Δ_1^* , Δ_2^* , Δ_3^* are unrelated to channel coefficient β .

The basic method is block matrix inversion: the fisher matrix in (9) can be considered as four 2×2 matrices in (29), where $\mathbf{A}(M, N)$, $\mathbf{B}(M, N, \beta)$, $\mathbf{D}(M, N, \beta)$ are defined as:

$$\mathbf{A}(M, N) \triangleq \begin{bmatrix} \|\mathbf{g}_k\|_2^2 & 0 \\ 0 & \|\mathbf{g}_k\|_2^2 \end{bmatrix}, \quad (30)$$

$$\mathbf{B}(M, N, \beta) \triangleq \begin{bmatrix} \text{Re}\{\mathbf{g}_k^H \tilde{\mathbf{g}}_{k,1}\} & \text{Re}\{\mathbf{g}_k^H \tilde{\mathbf{g}}_{k,2}\} \\ \text{Im}\{\mathbf{g}_k^H \tilde{\mathbf{g}}_{k,1}\} & \text{Im}\{\mathbf{g}_k^H \tilde{\mathbf{g}}_{k,2}\} \end{bmatrix}, \quad (31)$$

$$\mathbf{D}(M, N, \beta) \triangleq \begin{bmatrix} \|\tilde{\mathbf{g}}_{k,1}\|_2^2 & \text{Re}\{\tilde{\mathbf{g}}_{k,1}^H \tilde{\mathbf{g}}_{k,2}\} \\ \text{Re}\{\tilde{\mathbf{g}}_{k,1}^H \tilde{\mathbf{g}}_{k,2}\} & \|\tilde{\mathbf{g}}_{k,2}\|_2^2 \end{bmatrix}. \quad (32)$$

Then the inverse matrix of (29) is given in

$$\mathbf{I}(\Psi, \mathbf{W}_k)^{-1} = \frac{\sigma^2}{2|s_p|^2} \{ \mathbf{I}_{ip_1}(M, N) + \mathbf{I}_{ip_2}(M, N, \beta) \}, \quad (33)$$

where $\mathbf{I}_{ip_1}(M, N)$ and $\mathbf{I}_{ip_2}(M, N, \beta)$ are defined as

$$\mathbf{I}_{ip_1}(M, N) \triangleq \begin{bmatrix} \mathbf{A}(M, N) & \mathbf{0} \\ \mathbf{0} & \mathbf{0} \end{bmatrix} \quad (34)$$

$$\mathbf{I}_{ip_2}(M, N, \beta) \triangleq \begin{bmatrix} \mathbf{A}^{-1} \mathbf{B} \\ -\mathbf{J}_2 \end{bmatrix} (\mathbf{D} - \mathbf{B}^T \mathbf{A}^{-1} \mathbf{B})^{-1} [\mathbf{B}^T \mathbf{A}^{-1} - \mathbf{J}_2]. \quad (35)$$

\mathbf{J}_2 is 2×2 identity matrix. Combine (30), (31) and (32), $(\mathbf{D} - \mathbf{B}^T \mathbf{A}^{-1} \mathbf{B})/|\beta|^2$ can be simplified into a matrix unrelated to channel coefficient β , which is defined as:

$$\mathbf{I}_s(M, N) = \frac{(\mathbf{D} - \mathbf{B}^T \mathbf{A}^{-1} \mathbf{B})}{|\beta|^2}. \quad (36)$$

Therefore, we can rewrite (35) as:

$$\mathbf{I}_{ip_2}(M, N, \beta) = \begin{bmatrix} \mathbf{A}^{-1} \mathbf{B} \\ -\mathbf{J}_2 \end{bmatrix} (\beta^2 \mathbf{I}_s(M, N))^{-1} [\mathbf{B}^T \mathbf{A}^{-1} - \mathbf{J}_2]. \quad (37)$$

Except for the inverse of the Fisher information matrix, the other parts in (10) can be converted to (38), where $\bar{\beta}$ denotes the conjugate of β . Therefore, we rewrite (10) as:

$$\begin{aligned} \text{MSE}_{\text{opt}} &= \frac{1}{MN} \text{Tr} \left\{ (k \mathbf{I}(\Psi, \mathbf{W}^*))^{-1} \sum_{m=1}^M \sum_{n=1}^N (\mathbf{v}_{mn}^H \mathbf{v}_{mn}) \right\} \\ &= \frac{1}{kMN} \frac{\sigma^2}{2|s_p|^2} \text{Tr} \left\{ (\mathbf{I}(\Psi, \mathbf{W}^*))^{-1} \mathbf{T}(M, N, \beta) \right\} \\ &= \frac{1}{kMN} \frac{\sigma^2}{2|s_p|^2} \text{Tr} \{ \mathbf{I}_{ip_1}(M, N) \mathbf{T}(M, N, \beta) \} \\ &\quad + \frac{1}{kMN} \frac{\sigma^2}{2|s_p|^2} \text{Tr} \{ \mathbf{I}_{ip_2}(M, N) \mathbf{T}(M, N, \beta) \} \\ &\stackrel{(a)}{=} \frac{1}{kMN} \frac{\sigma^2}{2|s_p|^2} \left\{ \frac{2MN}{\|\mathbf{g}_k\|_2^2} + \text{Tr} \{ \mathbf{I}_{ip_2}(M, N) \mathbf{T}(M, N, \beta) \} \right\} \\ &= \frac{1}{k} \frac{\sigma^2}{2|s_p|^2} \left\{ \frac{2}{\|\mathbf{g}_k\|_2^2} + \frac{1}{MN} \text{Tr} \{ \mathbf{I}_{ip_2}(M, N) \mathbf{T}(M, N, \beta) \} \right\}, \end{aligned} \quad (39)$$

$$\begin{aligned} \mathbf{I}(\Psi, \mathbf{W}_k) &= \frac{2|s_p|^2}{\sigma^2} \begin{bmatrix} \|\mathbf{g}_k\|_2^2 & 0 & \text{Re}\{\mathbf{g}_k^H \tilde{\mathbf{g}}_{k_1}\} & \text{Re}\{\mathbf{g}_k^H \tilde{\mathbf{g}}_{k_2}\} \\ 0 & \|\mathbf{g}_k\|_2^2 & \text{Im}\{\mathbf{g}_k^H \tilde{\mathbf{g}}_{k_1}\} & \text{Im}\{\mathbf{g}_k^H \tilde{\mathbf{g}}_{k_2}\} \\ \text{Re}\{\mathbf{g}_k^H \tilde{\mathbf{g}}_{k_1}\} & \text{Im}\{\mathbf{g}_k^H \tilde{\mathbf{g}}_{k_1}\} & \|\tilde{\mathbf{g}}_{k_1}\|_2^2 & \text{Re}\{\tilde{\mathbf{g}}_{k_1}^H \tilde{\mathbf{g}}_{k_2}\} \\ \text{Re}\{\mathbf{g}_k^H \tilde{\mathbf{g}}_{k_2}\} & \text{Im}\{\mathbf{g}_k^H \tilde{\mathbf{g}}_{k_2}\} & \text{Re}\{\tilde{\mathbf{g}}_{k_1}^H \tilde{\mathbf{g}}_{k_2}\} & \|\tilde{\mathbf{g}}_{k_2}\|_2^2 \end{bmatrix} \\ &= \frac{2|s_p|^2}{\sigma^2} \begin{bmatrix} \mathbf{A}(M, N) & \mathbf{B}(M, N, \beta) \\ \mathbf{B}^T(M, N, \beta) & \mathbf{D}(M, N, \beta) \end{bmatrix}. \end{aligned} \quad (29)$$

$$\begin{aligned} T(M, N, \beta) &\triangleq \sum_{m=1}^M \sum_{n=1}^N (\mathbf{v}_{m,n}^H \mathbf{v}_{m,n}) \\ &= \begin{bmatrix} MN & jMN & j\pi\beta(M-1)N & j\pi\beta M(N-1) \\ -jMN & MN & \pi\beta(M-1)N & \pi\beta M(N-1) \\ -j\pi\bar{\beta}(M-1)N & \pi\bar{\beta}(M-1)N & \frac{2}{3}\pi^2|\beta|^2 \frac{(M-1)(2M-1)}{M}N & \pi^2|\beta|^2(M-1)(N-1) \\ -j\pi\bar{\beta}M(N-1) & \pi\bar{\beta}M(N-1) & \pi^2|\beta|^2(M-1)(N-1) & \frac{2}{3}\pi^2|\beta|^2 M \frac{(N-1)(2N-1)}{N} \end{bmatrix}. \end{aligned} \quad (38)$$

where step (a) is by combining (34) and (38).

Hence, $\text{Tr}\{\mathbf{I}_{ip_2}(M, N)\mathbf{T}(M, N, \beta)\}$ can be converted to

To calculate $\text{Tr}\{\mathbf{I}_{ip_2}(M, N)\mathbf{T}(M, N, \beta)\}$ in (39), we split $\mathbf{T}(M, N, \beta)$ in (38) into two parts (40):

$$\mathbf{T}(M, N, \beta) = MN \left\{ \begin{bmatrix} \mathbf{b}_T \\ \mathbf{c}_T \end{bmatrix} \begin{bmatrix} \mathbf{b}_T \\ \mathbf{c}_T \end{bmatrix}^H + \begin{bmatrix} \mathbf{0} & \mathbf{0} \\ \mathbf{0} & \mathbf{T}_D(M, N, \beta) \end{bmatrix} \right\}, \quad (40)$$

where \mathbf{b}_T , \mathbf{c}_T and $\mathbf{T}_D(M, N, \beta)$ are defined as:

$$\mathbf{b}_T \triangleq [1, -j]^T, \quad (41)$$

$$\mathbf{c}_T \triangleq \left[j\pi\bar{\beta} \frac{M-1}{M}, j\pi\bar{\beta} \frac{N-1}{N} \right]^T, \quad (42)$$

$$\begin{aligned} \text{Tr}\{\mathbf{I}_{ip_2}(M, N)\mathbf{T}(M, N, \beta)\} &= MN \left(\text{Tr} \left\{ \mathbf{I}_{ip_2}(M, N) \begin{bmatrix} \mathbf{b}_T \\ \mathbf{b}_T \end{bmatrix} \begin{bmatrix} \mathbf{b}_T \\ \mathbf{c}_T \end{bmatrix}^H \right\} \right) \\ &\quad + MN \left(\text{Tr} \left\{ \mathbf{I}_{ip_2}(M, N) \begin{bmatrix} \mathbf{0} & \mathbf{0} \\ \mathbf{0} & \mathbf{T}_D(M, N, \beta) \end{bmatrix} \right\} \right) \\ &= MN \left(\text{Tr} \left\{ \mathbf{I}_{ip_2}(M, N) \begin{bmatrix} \mathbf{b}_T \\ \mathbf{c}_T \end{bmatrix} \begin{bmatrix} \mathbf{b}_T \\ \mathbf{c}_T \end{bmatrix}^H \right\} \right) \\ &\quad + MN \left(\text{Tr} \left\{ \left(|\beta|^2 \mathbf{I}_s(M, N) \right)^{-1} \mathbf{T}_D(M, N, \beta) \right\} \right). \\ &= MN \left(\text{Tr} \left\{ \mathbf{I}_{ip_2}(M, N) \begin{bmatrix} \mathbf{b}_T \\ \mathbf{b}_T \end{bmatrix} \begin{bmatrix} \mathbf{b}_T \\ \mathbf{c}_T \end{bmatrix}^H \right\} \right) \\ &\quad + \frac{1}{3} \pi^2 \text{Tr} \left\{ \mathbf{I}_s(M, N)^{-1} \begin{bmatrix} \frac{(M-1)(M-3)}{M^2} & 0 \\ 0 & \frac{(N-1)(N-3)}{N^2} \end{bmatrix} \right\}. \end{aligned} \quad (44)$$

$$\mathbf{T}_D(M, N, \beta) \triangleq \frac{1}{3} \pi^2 |\beta|^2 \begin{bmatrix} \frac{(M-1)(M-3)}{M^2} & 0 \\ 0 & \frac{(N-1)(N-3)}{N^2} \end{bmatrix}. \quad (43)$$

Calculate the first part in (44), we obtain that

$$\begin{aligned}
& \text{Tr} \left\{ \mathbf{I}_{ip_2}(M, N) \begin{bmatrix} \mathbf{b}_T \\ \mathbf{c}_T \end{bmatrix} \begin{bmatrix} \mathbf{b}_T \\ \mathbf{c}_T \end{bmatrix}^H \right\} \\
&= \text{Tr} \left\{ \begin{bmatrix} \mathbf{A}^{-1}\mathbf{B} \\ -\mathbf{J}_2 \end{bmatrix} (|\beta|^2 \mathbf{I}_s(M, N))^{-1} [\mathbf{B}^T \mathbf{A}^{-1} - \mathbf{J}_2] \begin{bmatrix} \mathbf{b}_T \\ \mathbf{c}_T \end{bmatrix} \begin{bmatrix} \mathbf{b}_T \\ \mathbf{c}_T \end{bmatrix}^H \right\} \\
&= \text{Tr} \left\{ \begin{bmatrix} \mathbf{b}_T \\ \mathbf{c}_T \end{bmatrix}^H \begin{bmatrix} \mathbf{A}^{-1}\mathbf{B} \\ -\mathbf{J}_2 \end{bmatrix} (|\beta|^2 \mathbf{I}_s(M, N))^{-1} [\mathbf{B}^T \mathbf{A}^{-1} - \mathbf{J}_2] \begin{bmatrix} \mathbf{b}_T \\ \mathbf{c}_T \end{bmatrix} \right\} \\
&\stackrel{(a)}{=} \text{Tr} \left\{ (\beta \mathbf{a}_s(M, N))^H (|\beta|^2 \mathbf{I}_s(M, N))^{-1} \beta \mathbf{a}_s(M, N) \right\} \\
&= \text{Tr} \left\{ \left(\mathbf{a}_s^H(M, N) \right) (\mathbf{I}_s(M, N))^{-1} \mathbf{a}_s(M, N) \right\}, \tag{45}
\end{aligned}$$

where step (a) is due to the definition of $\mathbf{a}_s(M, N)$:

$$\begin{aligned}
\mathbf{a}_s(M, N) &\triangleq \frac{1}{\beta} \begin{bmatrix} \mathbf{B}^T \mathbf{A}^{-1} - \mathbf{J}_2 \end{bmatrix} \begin{bmatrix} \mathbf{b}_T \\ \mathbf{c}_T \end{bmatrix} \\
&= \frac{1}{\beta} \left(\frac{1}{\|\mathbf{g}_k\|_2^2} [\mathbf{g}_k^H \tilde{\mathbf{g}}_{k1}, \mathbf{g}_k^H \tilde{\mathbf{g}}_{k2}]^H - \mathbf{c}_T \right). \tag{46}
\end{aligned}$$

$\mathbf{a}_s(M, N)$ is unrelated to β by combining (9), (41) and (42). Substituting (45) into (44), we can obtain:

$$\begin{aligned}
& \text{Tr} \{ \mathbf{I}_{ip_2}(M, N) \mathbf{T}(M, N, \beta) \} \\
&= \text{Tr} \left\{ \mathbf{I}_{ip_2}(M, N) \begin{bmatrix} \mathbf{a}_T \\ \mathbf{b}_T \end{bmatrix} \begin{bmatrix} \mathbf{a}_T \\ \mathbf{b}_T \end{bmatrix}^H \right\} \\
&+ \text{Tr} \left\{ \mathbf{I}_{ip_2}(M, N) \begin{bmatrix} \mathbf{0} & \mathbf{0} \\ \mathbf{0} & \mathbf{T}_D(M, N, \beta) \end{bmatrix} \right\} \tag{47} \\
&= \text{Tr} \left\{ \mathbf{a}_s^H(M, N) \mathbf{I}_s(M, N)^{-1} \mathbf{a}_s(M, N) \right\} \\
&+ \text{Tr} \left\{ \mathbf{I}_s(M, N)^{-1} \frac{1}{3} \pi^2 \begin{bmatrix} \frac{(M-1)(M-3)}{M^2} & 0 \\ 0 & \frac{(N-1)(N-3)}{N^2} \end{bmatrix} \right\}.
\end{aligned}$$

which reveal that $\text{Tr} \{ \mathbf{I}_{ip_2}(M, N) \mathbf{T}(M, N, \beta) \}$ is irrelevant to channel coefficient β .

Since other parts in (39) are also irrelevant to channel β , the optimal channel vecotr MSE is unrelated to β and the optimal trial beam direction offsets have nothing to do with channel coefficient β .

Step 2: We prove that $\Delta_1^*, \Delta_2^*, \Delta_3^*$ are unrelated to normalized beam direction \mathbf{x} .

Consider the relationship between the optimal phase shifts and the real beam direction $\mathbf{x} = [x_1, x_2]^T$: if the phase shifts are steering vectors with $\mathbf{w}_{k,i} = \frac{1}{\sqrt{MN}} \mathbf{a}([x_1 + \delta_{k,i1}, x_2 + \delta_{k,i2}]^T)$, then the i -th ($i = 1, 2, 3$) element of \mathbf{g}_k and $\tilde{\mathbf{g}}_{k1}$ can be rewritten in (48) and (49).

$$\begin{aligned}
[\mathbf{g}_k]_i &= \frac{1}{\sqrt{MN}} \sum_{m=1}^M \sum_{n=1}^N e^{-j2\pi \left[\frac{(m-1)\delta_{k,i1}}{M} + \frac{(n-1)\delta_{k,i2}}{N} \right]} \tag{48} \\
&= \frac{1}{\sqrt{MN}} \frac{\sin(\pi\delta_{k,i1})}{\sin\left(\frac{\pi\delta_{k,i1}}{M}\right)} \frac{\sin(\pi\delta_{k,i2})}{\sin\left(\frac{\pi\delta_{k,i2}}{N}\right)} e^{-j\pi \left[\frac{M-1}{M} \delta_{k,i1} + \frac{N-1}{N} \delta_{k,i2} \right]}.
\end{aligned}$$

Since both \mathbf{g}_k and $\tilde{\mathbf{g}}_{k1}$ have nothing to do with the real beam direction $\mathbf{x} = [x_1, x_2]^T$ as shown in (48) and (49), which is also feasible to $\tilde{\mathbf{g}}_{k,2}$, the whole Fisher matrix has $\mathbf{I}(\Psi, \mathbf{W})$ has nothing to do with the real beam direction. In addition, $\mathbf{T}(M, N, \beta)$ in (38) is unrelated to the real beam direction. Therefore, the optimization of (10) has nothing to do with the beam direction. Therefore, the optimal trial beam direction offsets $\Delta_1^*, \Delta_2^*, \Delta_3^*$ are unrelated to the normalized beam direction $\mathbf{x} = [x_1, x_2]^T$.

Step 3: We prove that $\Delta_1^*, \Delta_2^*, \Delta_3^*$ converge as $M, N \rightarrow \infty$.

Let us go into the asymptotic features of (10). When antenna number $M, N \rightarrow +\infty$, the limit of i -th ($i = 1, 2, 3$) element of \mathbf{g}_k and $\tilde{\mathbf{g}}_{k,1}$ are given in (50) and (51).

$$\lim_{M, N \rightarrow +\infty} \frac{[\mathbf{g}_k]_i}{\sqrt{MN}} = \text{Sa}(\pi\delta_{k,i1}) \text{Sa}[\pi\delta_{k,i2}] e^{-j\pi(\delta_{k,i1} + \delta_{k,i2})}. \tag{50}$$

$$\begin{aligned}
& \lim_{M, N \rightarrow +\infty} \frac{[\tilde{\mathbf{g}}_{k1}]_i}{\sqrt{MN}} \tag{51} \\
&= j2\pi\beta \text{Sa}[\pi\delta_{k,i2}] e^{-j\pi\delta_{k,i2}} \frac{e^{-j2\pi\delta_{k,i1}} (1 + j2\pi\delta_{k,i1}) - 1}{(2\pi\delta_{k,i1})^2}.
\end{aligned}$$

By (50), we can obtain that

$$\lim_{M, N \rightarrow +\infty} \frac{\|\mathbf{g}_k\|_2^2}{MN} = \sum_{i=1}^3 \text{Sa}^2(\pi\delta_{k,i1}) \text{Sa}^2(\pi\delta_{k,i2}). \tag{52}$$

Hence, the first element of $\mathbf{I}(\Psi, \mathbf{W}_k)/MN$ in (9) is unrelated to antenna number when M and N tend to infinity. Similar to that, other elements of $\mathbf{I}(\Psi, \mathbf{W}_k)/MN$ in (9) are also unrelated to antenna number. Thus, we can define

$$\mathbf{I}_L(\Psi, \mathbf{W}_k) \triangleq \lim_{M, N \rightarrow +\infty} \frac{1}{MN} \mathbf{I}(\Psi, \mathbf{W}_k), \tag{53}$$

where $\mathbf{I}_L(\Psi, \mathbf{W}_k)$ is a matrix unrelated to M, N .

The limit of $\mathbf{T}(M, N, \beta)$ defined in (38) is given as follows:

$$\begin{aligned}
& \lim_{M, N \rightarrow +\infty} \frac{1}{MN} \mathbf{T}(M, N, \beta) \\
&= \begin{bmatrix} 1 & j & j\pi\beta & j\pi\beta \\ -j & 1 & \pi\beta & \pi\beta \\ -j\pi\bar{\beta} & \pi\bar{\beta} & \frac{4}{3}\pi^2|\beta|^2 & \pi^2|\beta|^2 \\ -j\pi\bar{\beta} & \pi\bar{\beta} & \pi^2|\beta|^2 & \frac{4}{3}\pi^2|\beta|^2 \end{bmatrix} \tag{54} \\
&\triangleq \mathbf{T}_L(\beta)
\end{aligned}$$

Combine (38), (53), and (54), we obtain the asymptotical MSE_{opt}

$$\begin{aligned}
& \lim_{M, N \rightarrow +\infty} (MN \times \text{MSE}_{\text{opt}}) \\
&= \lim_{M, N \rightarrow +\infty} \text{Tr} \left\{ (k\mathbf{I}(\Psi, \mathbf{W}^*))^{-1} \sum_{m=1}^M \sum_{n=1}^N \mathbf{v}_{mn}^H \mathbf{v}_{mn} \right\} \tag{55} \\
&= \lim_{M, N \rightarrow +\infty} \text{Tr} \left\{ (kMN\mathbf{I}_L(\Psi, \mathbf{W}_k))^{-1} MN\mathbf{T}_L(\beta) \right\} \\
&= \text{Tr} \left\{ (k\mathbf{I}_L(\Psi, \mathbf{W}_k))^{-1} \mathbf{T}_L(\beta) \right\}
\end{aligned}$$

$$\begin{aligned}
[\tilde{\mathbf{g}}_{k1}]_i &= \beta \mathbf{w}_{k,i}^H \frac{\partial \mathbf{a}(\mathbf{x})}{\partial x_1} = \frac{\beta}{\sqrt{MN}} \left(\sum_{m=1}^M \sum_{n=1}^N j2\pi \frac{m-1}{M} e^{-j2\pi \left[\frac{(m-1)\delta_{k,i1}}{M} + \frac{(n-1)\delta_{k,i2}}{N} \right]} \right) \\
&= \frac{j2\pi\beta}{M\sqrt{MN}} \left(\frac{\sin(\pi\delta_{k,i2})}{\sin\left(\frac{\pi\delta_{k,i2}}{N}\right)} e^{-j\pi \frac{N-1}{N} \delta_{k,i2}} \frac{(M-1)e^{-j2\pi \frac{M-1}{M} \delta_{k,i1}} - Me^{-j2\pi \frac{M-1}{M} \delta_{k,i1}} + 1}{\left[1 - e^{-j2\pi \frac{\delta_{k,i1}}{M}}\right]^2} e^{-j2\pi \frac{\delta_{k,i1}}{M}} \right). \tag{49}
\end{aligned}$$

as $M, N \rightarrow \infty$ in (55), which reveals that the optimal trial beam direction offsets $\Delta_1^*, \Delta_2^*, \Delta_3^*$ converge to determined values that are unrelated to array size M, N

Therefore, Lemma 3 gets proved.

APPENDIX D PROOF OF THEOREM 1

Recall the beam and channel tracking procedure in (17). We rewrite it as follows:

$$\hat{\Psi}_k = \hat{\Psi}_{k-1} + b_k \left(\mathbf{f}(\hat{\Psi}_{k-1}, \Psi_k) + \hat{\mathbf{z}}_k \right), \tag{56}$$

where $\mathbf{f}(\hat{\Psi}_{k-1}, \Psi_k)$ is defined as follows:

$$\begin{aligned}
\mathbf{f}(\hat{\Psi}_{k-1}, \Psi_k) &\triangleq \mathbb{E} \left[\mathbf{I}(\hat{\Psi}_{k-1}, \mathbf{W}_k)^{-1} \frac{\partial \log p(\mathbf{y}_k | \hat{\Psi}_{k-1}, \mathbf{W}_k)}{\partial \hat{\Psi}_{k-1}} \right] \\
&= \frac{2|s_p|^2}{\sigma^2} \mathbf{I}(\hat{\Psi}_{k-1}, \mathbf{W}_k)^{-1} \begin{bmatrix} \text{Re} \left\{ \mathbf{e}_k^H \left(\beta_k \mathbf{W}_k^H \mathbf{a}(\mathbf{x}_k) - \hat{\beta}_{k-1} \mathbf{e}_k \right) \right\} \\ \text{Im} \left\{ \mathbf{e}_k^H \left(\beta_k \mathbf{W}_k^H \mathbf{a}(\mathbf{x}_k) - \hat{\beta}_{k-1} \mathbf{e}_k \right) \right\} \\ \text{Re} \left\{ \tilde{\mathbf{e}}_{k1}^H \left(\beta_k \mathbf{W}_k^H \mathbf{a}(\mathbf{x}_k) - \hat{\beta}_{k-1} \mathbf{e}_k \right) \right\} \\ \text{Re} \left\{ \tilde{\mathbf{e}}_{k2}^H \left(\beta_k \mathbf{W}_k^H \mathbf{a}(\mathbf{x}_k) - \hat{\beta}_{k-1} \mathbf{e}_k \right) \right\} \end{bmatrix}, \tag{57}
\end{aligned}$$

and $\hat{\mathbf{z}}_k$ is given by

$$\begin{aligned}
\hat{\mathbf{z}}_k &\triangleq \mathbf{I}(\hat{\Psi}_{k-1}, \mathbf{W}_k)^{-1} \frac{\partial \log p(\mathbf{y}_k | \hat{\Psi}_{k-1}, \mathbf{W}_k)}{\partial \hat{\Psi}_{k-1}} - \mathbf{f}(\hat{\Psi}_{k-1}, \Psi_k) \\
&= \frac{2}{\sigma^2} \mathbf{I}(\hat{\Psi}_{k-1}, \mathbf{W}_k)^{-1} \begin{bmatrix} \text{Re} \{ s_p^H \mathbf{e}_k^H \mathbf{z}_k \} \\ \text{Im} \{ s_p^H \mathbf{e}_k^H \mathbf{z}_k \} \\ \text{Re} \{ s_p^H \tilde{\mathbf{e}}_{k1}^H \mathbf{z}_k \} \\ \text{Re} \{ s_p^H \tilde{\mathbf{e}}_{k2}^H \mathbf{z}_k \} \end{bmatrix}. \tag{58}
\end{aligned}$$

Since $\mathbf{z}_k \triangleq [z_{k,1}, z_{k,2}, z_{k,3}]$ is composed of three *i.i.d.* circularly symmetric complex Gaussian random variables, the expectation of $\hat{\mathbf{z}}_k$ is $\mathbb{E}[\hat{\mathbf{z}}_k] = \mathbf{0}$ and the covariance matrix is given by (59), where the step (a) are obtained as follows:

- Since $\mathbf{z}_k = [z_{k,1}, z_{k,2}, z_{k,3}]^T$ consists of three *i.i.d.* circularly symmetric complex Gaussian random variables, we get

$$s_p^H \mathbf{e}_k^H \mathbf{z}_k \sim \mathcal{CN}(0, \|s_p \mathbf{e}_k\|_2^2 \sigma^2), \tag{60}$$

$$s_p^H \tilde{\mathbf{e}}_{k1}^H \mathbf{z}_k \sim \mathcal{CN}(0, \|s_p \tilde{\mathbf{e}}_{k1}\|_2^2 \sigma^2). \tag{61}$$

$$s_p^H \tilde{\mathbf{e}}_{k2}^H \mathbf{z}_k \sim \mathcal{CN}(0, \|s_p \tilde{\mathbf{e}}_{k2}\|_2^2 \sigma^2). \tag{62}$$

- splitting the real part and imaginary part, we obtain

$$\begin{cases} \text{Re}\{s_p^H \mathbf{e}_k^H \mathbf{z}_k\} = \text{Re}\{s_p^H \mathbf{e}_k^H\} \text{Re}\{\mathbf{z}_k\} - \text{Im}\{s_p^H \mathbf{e}_k^H\} \text{Im}\{\mathbf{z}_k\}, \\ \text{Im}\{s_p^H \mathbf{e}_k^H \mathbf{z}_k\} = \text{Re}\{s_p^H \mathbf{e}_k^H\} \text{Im}\{\mathbf{z}_k\} + \text{Im}\{s_p^H \mathbf{e}_k^H\} \text{Re}\{\mathbf{z}_k\}, \\ \text{Re}\{s_p^H \tilde{\mathbf{e}}_{k1}^H \mathbf{z}_k\} = \text{Re}\{s_p^H \tilde{\mathbf{e}}_{k1}^H\} \text{Re}\{\mathbf{z}_k\} - \text{Im}\{s_p^H \tilde{\mathbf{e}}_{k1}^H\} \text{Im}\{\mathbf{z}_k\}, \\ \text{Re}\{s_p^H \tilde{\mathbf{e}}_{k2}^H \mathbf{z}_k\} = \text{Re}\{s_p^H \tilde{\mathbf{e}}_{k2}^H\} \text{Re}\{\mathbf{z}_k\} - \text{Im}\{s_p^H \tilde{\mathbf{e}}_{k2}^H\} \text{Im}\{\mathbf{z}_k\}, \\ \text{Re}\{s_p^H \mathbf{e}_k^H s_p \tilde{\mathbf{e}}_{k1}\} = |s_p|^2 \text{Re}\{\mathbf{e}_k^H \tilde{\mathbf{e}}_{k1}\} \\ \quad = \text{Re}\{s_p^H \mathbf{e}_k^H\} \text{Re}\{s_p \tilde{\mathbf{e}}_{k1}\} + \text{Im}\{s_p^H \mathbf{e}_k^H\} \text{Im}\{s_p \tilde{\mathbf{e}}_{k1}\}, \\ \text{Re}\{s_p^H \mathbf{e}_k^H s_p \tilde{\mathbf{e}}_{k2}\} = |s_p|^2 \text{Re}\{\mathbf{e}_k^H \tilde{\mathbf{e}}_{k2}\} \\ \quad = \text{Re}\{s_p^H \mathbf{e}_k^H\} \text{Re}\{s_p \tilde{\mathbf{e}}_{k2}\} + \text{Im}\{s_p^H \mathbf{e}_k^H\} \text{Im}\{s_p \tilde{\mathbf{e}}_{k2}\}, \\ \text{Im}\{s_p^H \mathbf{e}_k^H s_p \tilde{\mathbf{e}}_{k1}\} = |s_p|^2 \text{Im}\{\mathbf{e}_k^H \tilde{\mathbf{e}}_{k1}\} \\ \quad = \text{Re}\{s_p^H \mathbf{e}_k^H\} \text{Im}\{s_p \tilde{\mathbf{e}}_{k1}\} + \text{Im}\{s_p^H \mathbf{e}_k^H\} \text{Re}\{s_p \tilde{\mathbf{e}}_{k1}\}, \\ \text{Im}\{s_p^H \mathbf{e}_k^H s_p \tilde{\mathbf{e}}_{k2}\} = |s_p|^2 \text{Im}\{\mathbf{e}_k^H \tilde{\mathbf{e}}_{k2}\} \\ \quad = \text{Re}\{s_p^H \mathbf{e}_k^H\} \text{Im}\{s_p \tilde{\mathbf{e}}_{k2}\} + \text{Im}\{s_p^H \mathbf{e}_k^H\} \text{Re}\{s_p \tilde{\mathbf{e}}_{k2}\}, \\ \text{Re}\{s_p^H \tilde{\mathbf{e}}_{k1}^H s_p \tilde{\mathbf{e}}_{k2}\} = |s_p|^2 \text{Re}\{\tilde{\mathbf{e}}_{k1}^H \tilde{\mathbf{e}}_{k2}\} \\ \quad = \text{Re}\{s_p^H \tilde{\mathbf{e}}_{k1}^H\} \text{Re}\{s_p \tilde{\mathbf{e}}_{k2}\} + \text{Im}\{s_p^H \tilde{\mathbf{e}}_{k1}^H\} \text{Im}\{s_p \tilde{\mathbf{e}}_{k2}\} \end{cases} \tag{63}$$

- Combining (60), (61), (62) and (63), we can obtain

$$\begin{cases} \mathbb{E}[\text{Re}\{s_p^H \mathbf{e}_k^H \mathbf{z}_k\}^2] = \mathbb{E}[\text{Im}\{s_p^H \mathbf{e}_k^H \mathbf{z}_k\}^2] = \frac{|s_p|^2 \sigma^2}{2} \|\mathbf{e}_k\|_2^2, \\ \mathbb{E}[\text{Re}\{s_p^H \mathbf{e}_k^H \mathbf{z}_k\} \cdot \text{Im}\{s_p^H \mathbf{e}_k^H \mathbf{z}_k\}] = 0, \\ \mathbb{E}[\text{Re}\{s_p^H \mathbf{e}_k^H \mathbf{z}_k\} \cdot \text{Re}\{s_p^H \tilde{\mathbf{e}}_{k1}^H \mathbf{z}_k\}] = \frac{|s_p|^2 \sigma^2}{2} \text{Re}\{\mathbf{e}_k^H \tilde{\mathbf{e}}_{k1}\}, \\ \mathbb{E}[\text{Re}\{s_p^H \mathbf{e}_k^H \mathbf{z}_k\} \cdot \text{Re}\{s_p^H \tilde{\mathbf{e}}_{k2}^H \mathbf{z}_k\}] = \frac{|s_p|^2 \sigma^2}{2} \text{Re}\{\mathbf{e}_k^H \tilde{\mathbf{e}}_{k2}\}, \\ \mathbb{E}[\text{Im}\{s_p^H \mathbf{e}_k^H \mathbf{z}_k\} \cdot \text{Re}\{s_p^H \tilde{\mathbf{e}}_{k1}^H \mathbf{z}_k\}] = \frac{|s_p|^2 \sigma^2}{2} \text{Im}\{\mathbf{e}_k^H \tilde{\mathbf{e}}_{k1}\}, \\ \mathbb{E}[\text{Im}\{s_p^H \mathbf{e}_k^H \mathbf{z}_k\} \cdot \text{Re}\{s_p^H \tilde{\mathbf{e}}_{k2}^H \mathbf{z}_k\}] = \frac{|s_p|^2 \sigma^2}{2} \text{Im}\{\mathbf{e}_k^H \tilde{\mathbf{e}}_{k2}\}, \\ \mathbb{E}[\text{Re}\{s_p^H \tilde{\mathbf{e}}_{k1}^H \mathbf{z}_k\}^2] = \frac{|s_p|^2 \sigma^2}{2} \|\tilde{\mathbf{e}}_{k1}\|_2^2, \\ \mathbb{E}[\text{Re}\{s_p^H \tilde{\mathbf{e}}_{k2}^H \mathbf{z}_k\}^2] = \frac{|s_p|^2 \sigma^2}{2} \|\tilde{\mathbf{e}}_{k2}\|_2^2, \\ \mathbb{E}[\text{Re}\{s_p^H \tilde{\mathbf{e}}_{k1}^H \mathbf{z}_k\} \cdot \text{Re}\{s_p^H \tilde{\mathbf{e}}_{k2}^H \mathbf{z}_k\}] = \frac{|s_p|^2 \sigma^2}{2} \text{Re}\{\tilde{\mathbf{e}}_{k1}^H \tilde{\mathbf{e}}_{k2}\}. \end{cases} \tag{64}$$

$$\begin{aligned} \mathbb{E} \left[(\hat{\mathbf{z}}_k - \mathbb{E}[\hat{\mathbf{z}}_k]) (\hat{\mathbf{z}}_k - \mathbb{E}[\hat{\mathbf{z}}_k])^T \right] &= \frac{4}{\sigma^4} \mathbf{I} \left(\hat{\Psi}_{k-1}, \mathbf{W}_k \right)^{-1} \mathbb{E} \left\{ \begin{bmatrix} \text{Re}\{s_p^H \mathbf{e}_k^H \mathbf{z}_k\} \\ \text{Im}\{s_p^H \mathbf{e}_k^H \mathbf{z}_k\} \\ \text{Re}\{s_p^H \tilde{\mathbf{e}}_{k1}^H \mathbf{z}_k\} \\ \text{Re}\{s_p^H \tilde{\mathbf{e}}_{k2}^H \mathbf{z}_k\} \end{bmatrix} \begin{bmatrix} \text{Re}\{s_p^H \mathbf{e}_k^H \mathbf{z}_k\} \\ \text{Im}\{s_p^H \mathbf{e}_k^H \mathbf{z}_k\} \\ \text{Re}\{s_p^H \tilde{\mathbf{e}}_{k1}^H \mathbf{z}_k\} \\ \text{Re}\{s_p^H \tilde{\mathbf{e}}_{k2}^H \mathbf{z}_k\} \end{bmatrix}^T \right\} \mathbf{I} \left(\hat{\Psi}_{k-1}, \mathbf{W}_k \right)^{-1} \\ &\stackrel{(a)}{=} \mathbf{I} \left(\hat{\Psi}_{k-1}, \mathbf{W}_k \right)^{-1} \end{aligned} \quad (59)$$

Hence, we have

$$\mathbb{E} \left\{ \begin{bmatrix} \text{Re}\{s_p^H \mathbf{e}_k^H \mathbf{z}_k\} \\ \text{Im}\{s_p^H \mathbf{e}_k^H \mathbf{z}_k\} \\ \text{Re}\{s_p^H \tilde{\mathbf{e}}_{k1}^H \mathbf{z}_k\} \\ \text{Re}\{s_p^H \tilde{\mathbf{e}}_{k2}^H \mathbf{z}_k\} \end{bmatrix} \begin{bmatrix} \text{Re}\{s_p^H \mathbf{e}_k^H \mathbf{z}_k\} \\ \text{Im}\{s_p^H \mathbf{e}_k^H \mathbf{z}_k\} \\ \text{Re}\{s_p^H \tilde{\mathbf{e}}_{k1}^H \mathbf{z}_k\} \\ \text{Re}\{s_p^H \tilde{\mathbf{e}}_{k2}^H \mathbf{z}_k\} \end{bmatrix}^T \right\} = \frac{\sigma^4}{4} \mathbf{I}(\hat{\Psi}_{k-1}, \mathbf{W}_k). \quad (65)$$

- Substituting (65) into (59) yields the result of step (a).

Assume $\{\mathcal{G}_k : k \geq 0\}$ is an increasing sequence of σ -fields of $\{\hat{\Psi}_0, \hat{\Psi}_1, \hat{\Psi}_2, \dots\}$, i.e., $\mathcal{G}_{k-1} \subset \mathcal{G}_k$, where $\mathcal{G}_0 \triangleq \sigma(\hat{\Psi}_0)$ and $\mathcal{G}_k \triangleq \sigma(\hat{\Psi}_0, \hat{\mathbf{z}}_1, \dots, \hat{\mathbf{z}}_k)$ for $k \geq 1$. Because the $\hat{\mathbf{z}}_k$'s are composed of *i.i.d.* circularly symmetric complex Gaussian random variables with zero mean, $\hat{\mathbf{z}}_k$ is independent of \mathcal{G}_{k-1} , and $\hat{\Psi}_{k-1} \in \mathcal{G}_{k-1}$. Hence, we have

$$\begin{aligned} &\mathbb{E} \left[\mathbf{f} \left(\hat{\Psi}_{k-1}, \Psi \right) + \hat{\mathbf{z}}_k \middle| \mathcal{G}_{k-1} \right] \\ &= \mathbb{E} \left[\mathbf{f} \left(\hat{\Psi}_{k-1}, \Psi \right) \middle| \mathcal{G}_{k-1} \right] + \mathbb{E} \left[\hat{\mathbf{z}}_k \middle| \mathcal{G}_{k-1} \right] = \mathbf{f} \left(\hat{\Psi}_{k-1}, \Psi \right), \end{aligned} \quad (66)$$

for $k \geq 1$.

Theorem 5.2.1 in [27, Section 5.2.1] gives the conditions that ensure $\hat{\mathbf{x}}_k$ converges to a unique point when there are several points with probability one. Next, we will prove that if the step-size a_k is given by (18) with any $\varepsilon > 0$ and $K_0 \geq 0$, the recursive beam and channel tracking algorithm in (17) satisfies the corresponding conditions below:

- 1) Step-size requirements:

$$\begin{cases} a_k = \frac{\varepsilon}{k + K_0} \rightarrow 0, \\ \sum_{k=1}^{\infty} a_k = \sum_{k=1}^{\infty} \frac{\varepsilon}{k + K_0} = \infty, \\ \sum_{k=1}^{\infty} a_k^2 = \sum_{k=1}^{\infty} \frac{\varepsilon^2}{(k + K_0)^2} \leq \sum_{l=1}^{\infty} \frac{\varepsilon^2}{l^2} < \infty. \end{cases} \quad (67)$$

- 2) It is necessary to prove that $\sup_k \mathbb{E} \left[\left\| \mathbf{f} \left(\hat{\Psi}_{k-1}, \Psi \right) + \hat{\mathbf{z}}_k \right\|_2^2 \right] < \infty$.

From (56) and (59), we have

$$\begin{aligned} &\mathbb{E} \left[\left\| \mathbf{f} \left(\hat{\Psi}_{k-1}, \Psi \right) + \hat{\mathbf{z}}_k \right\|_2^2 \right] \\ &= \mathbb{E} \left[\left\| \mathbf{f} \left(\hat{\Psi}_{k-1}, \Psi \right) \right\|_2^2 + 2 \mathbf{f} \left(\hat{\Psi}_{k-1}, \Psi \right)^T \hat{\mathbf{z}}_k + \left\| \hat{\mathbf{z}}_k \right\|_2^2 \right] \\ &\stackrel{(a)}{=} \mathbb{E} \left[\left\| \mathbf{f} \left(\hat{\Psi}_{k-1}, \Psi \right) \right\|_2^2 \right] + \text{tr} \left\{ \mathbf{I}(\hat{\Psi}_{k-1}, \mathbf{W}_k)^{-1} \right\}, \end{aligned} \quad (68)$$

where step (a) is due to (59) and that $\hat{\mathbf{z}}_k$ is independent of $\mathbf{f} \left(\hat{\Psi}_{k-1}, \Psi \right)$.

From (57), we have

$$\begin{aligned} \left\| \mathbf{f} \left(\hat{\Psi}_{k-1}, \Psi \right) \right\|_2^2 &\leq \left\| \mathbf{I}(\hat{\Psi}_{k-1}, \mathbf{W}_k)^{-1} \right\|_F^2 \\ &\cdot \left\| \frac{2|s_p|^2}{\sigma^2} \begin{bmatrix} \text{Re} \left\{ \mathbf{e}_k^H \left(\beta_k \mathbf{W}_k^H \mathbf{a}(\mathbf{x}_k) - \hat{\beta}_{k-1} \mathbf{e}_k \right) \right\} \\ \text{Im} \left\{ \mathbf{e}_k^H \left(\beta_k \mathbf{W}_k^H \mathbf{a}(\mathbf{x}_k) - \hat{\beta}_{k-1} \mathbf{e}_k \right) \right\} \\ \text{Re} \left\{ \tilde{\mathbf{e}}_{k1}^H \left(\beta_k \mathbf{W}_k^H \mathbf{a}(\mathbf{x}_k) - \hat{\beta}_{k-1} \mathbf{e}_k \right) \right\} \\ \text{Re} \left\{ \tilde{\mathbf{e}}_{k2}^H \left(\beta_k \mathbf{W}_k^H \mathbf{a}(\mathbf{x}_k) - \hat{\beta}_{k-1} \mathbf{e}_k \right) \right\} \end{bmatrix} \right\|_2^2. \end{aligned} \quad (69)$$

As the Fisher information matrix is invertible, we get

$$\left\| \mathbf{I}(\hat{\Psi}_{k-1}, \mathbf{W}_k)^{-1} \right\|_F^2 < \infty. \quad (70)$$

Besides, $\mathbf{W}_k = [\mathbf{w}_{k,1}, \mathbf{w}_{k,2}, \mathbf{w}_{k,3}]$, $\mathbf{e}_k = \mathbf{W}_k^H \mathbf{a}(\hat{\mathbf{x}}_{k-1})$, $\tilde{\mathbf{e}}_{k1} = \mathbf{W}_k^H \frac{\partial \mathbf{a}(\hat{\mathbf{x}}_{k-1})}{\partial x_1}$, $\tilde{\mathbf{e}}_{k2} = \mathbf{W}_k^H \frac{\partial \mathbf{a}(\hat{\mathbf{x}}_{k-1})}{\partial x_2}$, hence we have

$$\begin{aligned} &\left| \mathbf{w}_{k,i}^H \mathbf{a}(\mathbf{x}) \right| \\ &= \left| \frac{1}{\sqrt{MN}} \sum_{m=1}^M \sum_{n=1}^N e^{-j2\pi \left(\frac{(m-1)\delta_{k,i1}}{M} + \frac{(n-1)\delta_{k,i2}}{N} \right)} \right| \\ &\leq \frac{1}{\sqrt{MN}} \sum_{m=1}^M \sum_{n=1}^N \left| e^{-j2\pi \left(\frac{(m-1)\delta_{k,i1}}{M} + \frac{(n-1)\delta_{k,i2}}{N} \right)} \right| \\ &= \sqrt{MN} < \infty \end{aligned} \quad (71)$$

$$\begin{aligned} &\left| \mathbf{w}_{k,i}^H \frac{\partial \mathbf{a}(\mathbf{x})}{\partial x_1} \right| \\ &= \left| \frac{1}{\sqrt{MN}} \sum_{m=1}^M \sum_{n=1}^N j2\pi \frac{m-1}{M} e^{-j2\pi \left(\frac{(m-1)\delta_{k,i1}}{M} + \frac{(n-1)\delta_{k,i2}}{N} \right)} \right| \\ &\leq \frac{2\pi}{M\sqrt{MN}} \sum_{m=1}^M \sum_{n=1}^N (m-1) \left| e^{-j2\pi \left(\frac{(m-1)\delta_{k,i1}}{M} + \frac{(n-1)\delta_{k,i2}}{N} \right)} \right| \\ &= \sqrt{MN} (M-1) < \infty \end{aligned} \quad (72)$$

and

$$\begin{aligned}
& \left| \mathbf{w}_{k,i}^H \frac{\partial \mathbf{a}(\mathbf{x})}{\partial x_2} \right| \\
&= \left| \frac{1}{\sqrt{MN}} \sum_{m=1}^M \sum_{n=1}^N j2\pi \frac{n-1}{N} e^{-j2\pi \left(\frac{(m-1)\delta_{k,i1}}{M} + \frac{(n-1)\delta_{k,i2}}{N} \right)} \right| \\
&\leq \frac{2\pi}{N\sqrt{MN}} \sum_{m=1}^M \sum_{n=1}^N (n-1) \left| e^{-j2\pi \left(\frac{(m-1)\delta_{k,i1}}{M} + \frac{(n-1)\delta_{k,i2}}{N} \right)} \right| \\
&= \sqrt{MN} (N-1) < \infty
\end{aligned} \tag{73}$$

for $i = 1, 2, 3$ and all possible $\mathbf{w}_{k,i}$ and \mathbf{x} , thus we can get

$$\left\| \frac{2|s_p|^2}{\sigma^2} \begin{bmatrix} \text{Re} \left\{ \mathbf{e}_k^H \left(\beta_k \mathbf{W}_k^H \mathbf{a}(\mathbf{x}_k) - \hat{\beta}_{k-1} \mathbf{e}_k \right) \right\} \\ \text{Im} \left\{ \mathbf{e}_k^H \left(\beta_k \mathbf{W}_k^H \mathbf{a}(\mathbf{x}_k) - \hat{\beta}_{k-1} \mathbf{e}_k \right) \right\} \\ \text{Re} \left\{ \tilde{\mathbf{e}}_{k1}^H \left(\beta_k \mathbf{W}_k^H \mathbf{a}(\mathbf{x}_k) - \hat{\beta}_{k-1} \mathbf{e}_k \right) \right\} \\ \text{Re} \left\{ \tilde{\mathbf{e}}_{k2}^H \left(\beta_k \mathbf{W}_k^H \mathbf{a}(\mathbf{x}_k) - \hat{\beta}_{k-1} \mathbf{e}_k \right) \right\} \end{bmatrix} \right\|_2 < \infty. \tag{74}$$

Hence, combining (70) and (74), we have

$$\mathbb{E} \left[\left\| \mathbf{f}(\hat{\psi}_{n-1}, \psi) \right\|_2^2 \right] < \infty. \tag{75}$$

According to (70), it is clear that $\text{tr} \left\{ \mathbf{I}(\hat{\Psi}_{k-1}, \mathbf{W}_k)^{-1} \right\} < \infty$. Then, we can get that

$$\sup_n \mathbb{E} \left[\left\| \mathbf{f}(\hat{\Psi}_{k-1}, \Psi) + \hat{\mathbf{z}}_k \right\|_2^2 \right] < \infty. \tag{76}$$

3) The function $\mathbf{f}(\hat{\Psi}_{k-1}, \Psi)$ should be continuous with respect to $\hat{\Psi}_{k-1}$.

By using (57), we know that each element of $\mathbf{f}(\hat{\Psi}_{k-1}, \Psi)$ is continuous with respect to $\hat{\Psi}_{k-1} = [\hat{\beta}_{re}, \hat{\beta}_{im}, \hat{x}_1, \hat{x}_2]^T$. Therefore, $\mathbf{f}(\hat{\Psi}_{k-1}, \Psi)$ is continuous with respect to $\hat{\Psi}_{k-1}$.

4) Let $\gamma_k = \mathbb{E} \left[\mathbf{f}(\hat{\Psi}_{k-1}, \Psi) + \hat{\mathbf{z}}_k \mid \mathcal{G}_{k-1} \right] - \mathbf{f}(\hat{\Psi}_{k-1}, \Psi)$. We need to prove that $\sum_{k=1}^{\infty} \|b_k \gamma_k\|_2 < \infty$ with probability one.

From (66), we get $\gamma_k = \mathbf{0}$ for all $k \geq 1$. So we have $\sum_{k=1}^{\infty} \|b_k \gamma_k\|_2 = 0 < \infty$ with probability one.

By Theorem 5.2.1 in [27], $\hat{\mathbf{x}}_k$ converges to a unique stable point within the stable points set with probability one.

APPENDIX E PROOF OF THEOREM 2

Theorem E is proven in three steps:

Step 1: Two continuous processes based on the discrete process $\hat{\Psi}_k = [\hat{\beta}_k^{re}, \hat{\beta}_k^{im}, \hat{x}_{k,1}, \hat{x}_{k,2}]^T$ are established here, i.e., $\bar{\Psi}(t) \triangleq [\bar{\beta}^{re}(t), \bar{\beta}^{im}(t), \bar{x}_1(t), \bar{x}_2(t)]^T$ and $\tilde{\Psi}^k(t) \triangleq [\tilde{\beta}^{re,k}(t), \tilde{\beta}^{im,k}(t), \tilde{x}_1^k(t), \tilde{x}_2^k(t)]^T$.

The discrete time parameters are defined as: $t_0 \triangleq 0$, $t_k \triangleq \sum_{i=1}^k b_i$, $k \geq 1$. The first continuous process $\bar{\Psi}(t)$, $t \geq 0$ is

constructed as the linear interpolation of the sequence $\hat{\Psi}_k$, $k \geq 0$, where $\bar{\Psi}(t_k) = \hat{\Psi}_k$, $k \geq 0$. Therefore, $\bar{\Psi}(t)$ is given by

$$\bar{\Psi}(t) = \bar{\Psi}(t_k) + \frac{(t-t_k)}{b_{k+1}} [\bar{\Psi}(t_{k+1}) - \bar{\Psi}(t_k)], \quad t \in [t_k, t_{k+1}]. \tag{77}$$

The second continuous process $\tilde{\Psi}^k(t)$ is the solution of the following ordinary differential equation (ODE):

$$\frac{d\tilde{\Psi}^k(t)}{dt} = \mathbf{f}(\tilde{\Psi}^k(t), \Psi), \tag{78}$$

for $t \in [t_k, \infty)$, where $\tilde{\Psi}^k(t_k) = \bar{\Psi}(t_k) = \hat{\Psi}_k$, $k \geq 0$. Thus, $\tilde{\Psi}^k(t)$ can be given as

$$\tilde{\Psi}^k(t) = \bar{\Psi}(t_k) + \int_{t_k}^t \mathbf{f}(\tilde{\Psi}^k(v), \Psi) dv, \quad t \geq t_k. \tag{79}$$

Step 2: By using the two continuous processes $\bar{\Psi}(t)$ and $\tilde{\Psi}^k(t)$ constructed in step 1, a sufficient condition for the convergence of the discrete process $\hat{\mathbf{x}}_k$ is provided here.

We first construct a time-invariant set \mathcal{I} that includes the real direction \mathbf{x} within the mainlobe, i.e., $\mathbf{x} \in \mathcal{I} \subset \mathcal{B}(\mathbf{x})^3$. Define $\tilde{\mathbf{x}}^0(t) \triangleq [\tilde{x}_1^0(t), \tilde{x}_2^0(t)]^T$ and denote $\hat{\mathbf{x}}_b = \tilde{\mathbf{x}}^0(t_b)$ as the beam direction of the process $\tilde{\Psi}^0(t)$ that is closest to the boundary of the mainlobe, which is given by

$$\inf_{\mathbf{v} \in \partial \mathcal{B}(\mathbf{x}), t \geq 0} \|\mathbf{v} - \tilde{\mathbf{x}}^0(t)\|_2 = \inf_{\mathbf{v} \in \partial \mathcal{B}(\mathbf{x})} \|\mathbf{v} - \hat{\mathbf{x}}_b\|_2 > 0. \tag{80}$$

Then we pick δ such that

$$\min \left\{ \inf_{\mathbf{v} \in \partial \mathcal{B}(\mathbf{x})} \|\mathbf{v} - \hat{\mathbf{x}}_b\|_{-\infty}, \|\hat{\mathbf{x}}_b - \mathbf{x}\|_{-\infty} \right\} > \delta > 0, \tag{81}$$

where $\|\mathbf{u}\|_{-\infty} = \min_{l=1,2} [\mathbf{u}]_l$ denotes the minimum element of \mathbf{u} .

Note that when $t \geq t_b$, the solution $\tilde{\Psi}^0(t)$ of the ODE (78) will approach the real channel coefficient β and beam direction \mathbf{x} monotonically as time t increases. Hence, we construct the invariant set \mathcal{I} as (82). An example of the invariant set \mathcal{I} is shown in Fig. 7.

Then, a sufficient condition will be established in Lemma 4 that ensures $\hat{\mathbf{x}}_k \in \mathcal{I}$ for $k \geq 0$, and hence from Corollary 2.5 in [26], we can obtain that $\hat{\mathbf{x}}_k$ converges to \mathbf{x} . Before giving Lemma 4, let us provide some definitions first:

- Pick $T > 0$ such that the solution $\tilde{\Psi}^0(t)$, $t \geq 0$ of the ODE (78) with $\tilde{\Psi}^0(0) = [\hat{\beta}_0^{re}, \hat{\beta}_0^{im}, \hat{x}_{0,1}, \hat{x}_{0,2}]^T$ satisfies $\inf_{\mathbf{v} \in \partial \mathcal{B}} \|\mathbf{v} - \tilde{\mathbf{x}}^0(t)\| \geq 2\delta$ for $t \geq T$. Since when $t \geq t_b$, $\tilde{\mathbf{x}}^0(t)$ will approach the real beam direction \mathbf{x} monotonically as time t increases, one possible T is given by

$$T = \arg \min_{t \in [t_b, \infty)} \left| \left| \int_{t_b}^t \mathbf{f}(\tilde{\Psi}^0(v), \Psi) dv \right|_3 - \delta \right|, \tag{83}$$

where $[\cdot]_i$ obtains the i -th element of the vector.

- Let $T_0 \triangleq 0$ and $T_{l+1} \triangleq \min \{t_i : t_i \geq T_l + T, i \geq 0\}$ for $l \geq 0$. Then $T_{l+1} - T_l \in [T, T + b_1]$ and $T_l = t_{\tilde{k}(l)}$ for

³The boundary of the set $\mathcal{B}(\mathbf{x})$ is denoted by $\partial \mathcal{B}(\mathbf{x})$.

$$\mathcal{I} = \left(x_1 - |x_1 - \hat{x}_{1,b}| - \delta, x_1 + |x_1 - \hat{x}_{1,b}| + \delta \right) \times \left(x_2 - |x_2 - \hat{x}_{2,b}| - \delta, x_2 + |x_2 - \hat{x}_{2,b}| + \delta \right) \subset \mathcal{B}(\mathbf{x}). \quad (82)$$

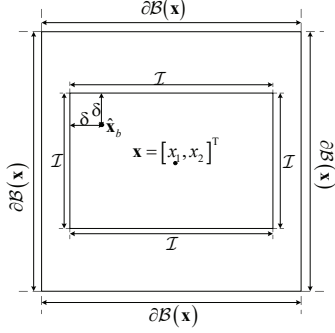


Fig. 7. An illustration of the invariant set \mathcal{I} .

some $\tilde{k}(l) \uparrow \infty$, where $\tilde{k}(0) = 0$. Let $\tilde{\Psi}^{\tilde{k}(l)}(t)$ denote the solution of ODE (78) for $t \in I_l \triangleq [T_l, T_{l+1}]$ with $\tilde{\Psi}^{\tilde{k}(l)}(T_l) = \tilde{\Psi}(T_l)$, $l \geq 0$.

Hence, we can obtain the following lemma:

Lemma 4. If $\sup_{t \in I_l} \|\bar{\mathbf{x}}(t) - \tilde{\mathbf{x}}^{\tilde{k}(l)}(t)\|_2 \leq \delta$ for all $l \geq 0$, then $\hat{\mathbf{x}}_k \in \mathcal{I}$ for all $k \geq 0$.

Proof. If $\sup_{t \in I_l} \|\bar{\mathbf{x}}(t) - \tilde{\mathbf{x}}^{\tilde{k}(l)}(t)\|_2 \leq \delta$ for all $l \geq 0$, then $\sup_{t \in I_l} \|\bar{x}_1(t) - \tilde{x}_1^{\tilde{k}(l)}(t)\|_2 \leq \delta$ and $\sup_{t \in I_l} \|\bar{x}_2(t) - \tilde{x}_2^{\tilde{k}(l)}(t)\|_2 \leq \delta$.

According to Lemma 1 in [17], $\hat{x}_{k,1} \in \mathcal{I}$ for all $k \geq 0$ and $\hat{x}_{k,2} \in \mathcal{I}$ for all $k \geq 0$. Hence, $\hat{\mathbf{x}}_k \in \mathcal{I}$ for all $k \geq 0$. ■

Step 3: We will derive the probability lower bound for the condition in Lemma 4, which is also a lower bound for $P(\hat{\mathbf{x}}_k \rightarrow \mathbf{x} | \hat{\mathbf{x}}_0 \in \mathcal{B}(\mathbf{x}))$.

We will derive the probability lower bound for the condition in Lemma 4, which results in the following lemma:

Lemma 5. If (i) the initial point satisfies $\hat{\mathbf{x}}_0 \in \mathcal{B}(\mathbf{x})$, (ii) b_k is given by (18) with any $\epsilon > 0$, then there exist $K_0 \geq 0$ and $C > 0$ such that

$$P(\hat{\mathbf{x}}_k \in \mathcal{I}, \forall k \geq 0) \geq 1 - 8e^{-\frac{C|s_p|^2}{\epsilon^2 \sigma^2}}. \quad (84)$$

Proof. See Appendix G. ■

Finally, by applying Lemma 5 and Corollary 2.5 in [26], we can obtain

$$P(\hat{\mathbf{x}}_k \rightarrow \mathbf{x} | \hat{\mathbf{x}}_0 \in \mathcal{B}) \geq P(\hat{\mathbf{x}}_k \in \mathcal{I}, \forall k \geq 0) \geq 1 - 8e^{-\frac{C|s_p|^2}{\epsilon^2 \sigma^2}}, \quad (85)$$

which completes the proof of Theorem E.

APPENDIX F PROOF OF THEOREM 3

If the step-size b_k is given by (18) with any $\epsilon > 0$ and $K_0 \geq 0$, the sufficient conditions are provided by Theorem 6.6.1 [24, Section 6.6] to prove the asymptotic normality of $\sqrt{k}(\hat{\mathbf{x}}_k - \mathbf{x})$, i.e., $\sqrt{k}(\hat{\mathbf{x}}_k - \mathbf{x}) \xrightarrow{d} \mathcal{N}(0, \Sigma_{\mathbf{x}})$. With the condition that $\hat{\Psi}_k \rightarrow \Psi$, we can prove that the recursive beam and channel tracking algorithm satisfies the condition above and obtain the variance Σ as follows:

- 1) Equation (56) is supposed to satisfy: (i) there exists an increasing sequence of σ -fields $\{\mathcal{F}_k : k \geq 0\}$ such that $\mathcal{F}_l \subset \mathcal{F}_k$ for $l < k$, and (ii) the random noise $\hat{\mathbf{z}}_k$ is \mathcal{F}_k -measurable and independent of \mathcal{F}_{k-1} .

As is shown in Appendix D, there exists an increasing sequence of σ -fields $\{\mathcal{G}_k : k \geq 0\}$, where $\hat{\mathbf{z}}_k$ is measurable with respect to \mathcal{G}_k , i.e., $\mathbb{E}[\hat{\mathbf{z}}_k | \mathcal{G}_k] = \hat{\mathbf{z}}_k$, and is independent of \mathcal{G}_{k-1} , i.e., $\mathbb{E}[\hat{\mathbf{z}}_k | \mathcal{G}_{k-1}] = \mathbb{E}[\hat{\mathbf{z}}_k] = 0$.

- 2) $\hat{\mathbf{x}}_k$ should converge to \mathbf{x} almost surely as $k \rightarrow \infty$.

We assume that $\hat{\Psi}_k \rightarrow \Psi$, hence $\hat{\mathbf{x}}_k$ converges to \mathbf{x} almost surely when $k \rightarrow \infty$.

- 3) The stable condition:

In (57), we rewrite $\mathbf{f}(\hat{\Psi}_{k-1}, \Psi)$ as follows:

$$\mathbf{f}(\hat{\Psi}_{k-1}, \Psi) = \mathbf{C}_1 (\hat{\Psi}_{k-1} - \Psi) + \begin{bmatrix} o(\|\hat{\Psi}_{k-1} - \Psi\|_2) \\ o(\|\hat{\Psi}_{k-1} - \Psi\|_2) \\ o(\|\hat{\Psi}_{k-1} - \Psi\|_2) \end{bmatrix}, \quad (86)$$

, where \mathbf{C}_1 is given by

$$\mathbf{C}_1 = \frac{\partial \mathbf{f}(\hat{\Psi}_{k-1}, \Psi)}{\partial \hat{\Psi}_{k-1}^T} \bigg|_{\hat{\Psi}_{k-1} = \Psi} = - \begin{bmatrix} 1 & 0 & 0 \\ 0 & 1 & 0 \\ 0 & 0 & 1 \end{bmatrix}. \quad (87)$$

Then the stable condition is obtained that:

$$\mathbf{E} = \mathbf{C}_1 \cdot \epsilon + \frac{1}{2} = - \begin{bmatrix} \epsilon - \frac{1}{2} & 0 & 0 \\ 0 & \epsilon - \frac{1}{2} & 0 \\ 0 & 0 & \epsilon - \frac{1}{2} \end{bmatrix} \prec 0, \quad (88)$$

which leads to $\epsilon > \frac{1}{2}$.

- 4) The noise vector $\hat{\mathbf{z}}_k$ satisfies:

$$\mathbb{E}[\|\hat{\mathbf{z}}_k\|_2^2] = \text{tr}(\mathbf{I}(\hat{\Psi}_{k-1}, \mathbf{W}_k)^{-1}) < \infty, \quad (89)$$

and

$$\lim_{v \rightarrow \infty} \sup_{k \geq 1} \int_{\|\hat{\mathbf{z}}_k\|_2 > v} \|\hat{\mathbf{z}}_k\|_2^2 p(\hat{\mathbf{z}}_k) d\hat{\mathbf{z}}_k = 0. \quad (90)$$

Let

$$\begin{aligned} \mathbf{F} &= \lim_{k \rightarrow \infty} \mathbb{E} [\hat{\mathbf{z}}_k \hat{\mathbf{z}}_k^T] \\ \hat{\Psi}_k &\rightarrow \Psi \\ &\stackrel{(a)}{=} \lim_{k \rightarrow \infty} \mathbf{I}(\hat{\Psi}_k, \mathbf{W}_{k+1})^{-1} = \mathbf{I}(\Psi, \mathbf{W}^*)^{-1}, \\ \hat{\Psi}_k &\rightarrow \Psi \end{aligned} \quad (91)$$

where step (a) is obtained from (59).

By Theorem 6.6.1 [24, Section 6.6], we have

$$\sqrt{k + K_0} (\hat{\Psi}_k - \Psi) \xrightarrow{d} \mathcal{N}(0, \Sigma),$$

where

$$\begin{aligned} \Sigma &= \alpha^2 \cdot \int_0^\infty e^{\mathbf{E}v} \mathbf{F} e^{\mathbf{E}^H v} dv \\ &= \frac{\varepsilon^2}{2\varepsilon - 1} \mathbf{I}(\Psi, \mathbf{W}^*)^{-1}. \end{aligned} \quad (92)$$

Due to that $\lim_{k \rightarrow \infty} \sqrt{(k + K_0)/k} = 1$, we have

$$\sqrt{k} (\hat{\Psi}_k - \Psi) \rightarrow \sqrt{k} \cdot \sqrt{\frac{k + K_0}{k}} (\hat{\Psi}_k - \Psi) \xrightarrow{d} \mathcal{N}(0, \Sigma),$$

if $k \rightarrow \infty$. Thus, we can get

$$\sqrt{k} (\hat{\Psi}_k - \Psi) \xrightarrow{d} \mathcal{N}(0, \Sigma). \quad (93)$$

By adapting $\alpha = 1$ in (92), we can obtain

$$\sqrt{k} (\hat{\Psi}_k - \Psi) \xrightarrow{d} \mathcal{N}(0, \mathbf{I}(\psi, \mathbf{W}^*)^{-1}). \quad (94)$$

Combining (26), (94) and (10), we can conclude that

$$\lim_{k \rightarrow \infty} k \mathbb{E} \left[\left\| \hat{\beta}_k \mathbf{a}(\hat{\mathbf{x}}_k) - \beta_k \mathbf{a}(\mathbf{x}_k) \right\|_2^2 \right] = u(\Psi, \mathbf{W}^*) = \text{MSE}_{\text{opt}}. \quad (95)$$

APPENDIX G PROOF OF LEMMA 5

The following lemmas are introduced to prove Lemma 5.

Lemma 6 (Lemma 3 [17]). Given T by (83) and

$$k_T \triangleq \inf \{i \in \mathbb{Z} : t_{k+i} \geq t_k + T\}. \quad (96)$$

If there exists a constant $C > 0$, which satisfies

$$\begin{aligned} &\left\| \bar{\Psi}(t_{k+l}) - \tilde{\Psi}^k(t_{k+l}) \right\|_2 \\ &\leq L \sum_{i=1}^l a_{k+i} \left\| \bar{\Psi}(t_{k+i-1}) - \tilde{\Psi}^k(t_{k+i-1}) \right\|_2 + C, \end{aligned} \quad (97)$$

for all $k \geq 0$ and $1 \leq l \leq k_T$, then

$$\sup_{t \in [t_k, t_{k+k_T}]} \left\| \bar{\Psi}(t) - \tilde{\Psi}^k(t) \right\|_2 \leq \frac{C_{\mathbf{f}} b_{k+1}}{2} + C e^{L(T+b_1)}, \quad (98)$$

where L and $C_{\mathbf{f}}$ are defined in (103) and (104) separately.

Lemma 7 (Lemma 4 [15]). If $\{M_i : i = 1, 2, \dots\}$ satisfies that: (i) M_i is Gaussian distributed with zero mean, and (ii) M_i is a martingale in i , then

$$P \left(\sup_{0 \leq i \leq k} |M_i| > \eta \right) \leq 2 \exp \left\{ -\frac{\eta^2}{2 \text{Var}[M_k]} \right\}, \quad (99)$$

for any $\eta > 0$.

Lemma 8 (Lemma 5 [15]). If given a constant $C > 0$, then

$$G(v) = \frac{1}{v} \exp \left[-\frac{C}{v} \right], \quad (100)$$

is increasing for all $0 < v < C$.

Let $\xi_0 \triangleq \mathbf{0}$ and $\xi_k \triangleq \sum_{l=1}^k a_l \hat{\mathbf{z}}_l$, $k \geq 1$, where $\hat{\mathbf{z}}_l$ is given in (58). With (77) and (79), we have for t_{k+l} , $1 \leq l \leq k_T$,

$$\begin{aligned} \bar{\psi}(t_{k+l}) &= \bar{\psi}(t_k) + \sum_{i=1}^l a_{k+i} \mathbf{f}(\bar{\psi}(t_{k+i-1}), \psi) \\ &\quad + (\xi_{k+l} - \xi_k), \end{aligned} \quad (101)$$

and

$$\begin{aligned} \tilde{\psi}^n(t_{k+l}) &= \tilde{\psi}^k(t_k) + \int_{t_k}^{t_{k+l}} \mathbf{f}(\tilde{\psi}^k(v), \psi) dv \\ &= \tilde{\psi}^k(t_k) + \sum_{i=1}^l a_{k+i} \mathbf{f}(\tilde{\psi}^k(t_{k+i-1}), \psi) \\ &\quad + \int_{t_k}^{t_{k+l}} \left[\mathbf{f}(\tilde{\psi}^k(v), \psi) - \mathbf{f}(\tilde{\psi}^k(\underline{v}), \psi) \right] dv, \end{aligned} \quad (102)$$

where $\underline{v} \triangleq \max \{t_k : t_k \leq v, k \geq 0\}$ for $v \geq 0$.

To bound $\int_{t_k}^{t_{k+l}} \left[\mathbf{f}(\tilde{\psi}^k(v), \psi) - \mathbf{f}(\tilde{\psi}^k(\underline{v}), \psi) \right] dv$ on the RHS of (102), we obtain the Lipschitz constant of function $\mathbf{f}(\mathbf{v}, \psi)$ considering the first variable \mathbf{v} , given by

$$L \triangleq \sup_{\mathbf{v}_1 \neq \mathbf{v}_2} \frac{\|\mathbf{f}(\mathbf{v}_1, \psi) - \mathbf{f}(\mathbf{v}_2, \psi)\|_2}{\|\mathbf{v}_1 - \mathbf{v}_2\|_2}. \quad (103)$$

Similar to (69), for any $t \geq t_k$, we can obtain that there exists a constant $0 < C_{\mathbf{f}} < \infty$ such that

$$\left\| \mathbf{f}(\tilde{\psi}^k(t), \psi) \right\|_2 \leq C_{\mathbf{f}}. \quad (104)$$

Hence, we have

$$\begin{aligned}
& \left\| \int_{t_k}^{t_{k+m}} \left[\mathbf{f}(\tilde{\psi}^k(v), \psi) - \mathbf{f}(\tilde{\psi}^k(\underline{v}), \psi) \right] dv \right\|_2 \\
& \leq \int_{t_k}^{t_{k+l}} \left\| \mathbf{f}(\tilde{\psi}^k(v), \psi) - \mathbf{f}(\tilde{\psi}^k(\underline{v}), \psi) \right\|_2 dv \\
& \stackrel{(a)}{\leq} \int_{t_k}^{t_{k+l}} L \left\| \tilde{\psi}^k(v) - \tilde{\psi}^k(\underline{v}) \right\|_2 dv \\
& \stackrel{(b)}{\leq} \int_{t_k}^{t_{k+l}} L \left\| \int_{\underline{v}}^v \mathbf{f}(\tilde{\psi}^k(s), \psi) ds \right\|_2 dv \\
& \leq \int_{t_k}^{t_{k+l}} \int_{\underline{v}}^v L \left\| \mathbf{f}(\tilde{\psi}^k(s), \psi) \right\|_2 ds dv \\
& \stackrel{(c)}{\leq} \int_{t_k}^{t_{k+l}} \int_{\underline{v}}^v C_{\mathbf{f}} L ds dv = \int_{t_k}^{t_{k+l}} C_{\mathbf{f}} L (v - \underline{v}) dv \\
& = \sum_{i=1}^l \int_{t_{k+i-1}}^{t_{k+i}} C_{\mathbf{f}} L (v - t_{k+i-1}) dv \\
& = \sum_{i=1}^l \frac{C_{\mathbf{f}} L (t_{k+i} - t_{k+i-1})^2}{2} = \frac{C_{\mathbf{f}} L}{2} \sum_{i=1}^l b_{k+i}^2,
\end{aligned} \tag{105}$$

where step (a) is due to (103), step (b) is due to the definition in (79), and step (c) is due to (104). Then, by subtracting $\tilde{\psi}^k(t_{k+l})$ in (102) from $\tilde{\psi}(t_{k+l})$ in (101) and taking norms, the following inequality can be obtained from (103) and (105) for $k \geq 0, 1 \leq l \leq k_T$:

$$\begin{aligned}
& \left\| \tilde{\psi}(t_{k+l}) - \tilde{\psi}^k(t_{k+l}) \right\|_2 \\
& \leq L \sum_{i=1}^l b_{k+i} \left\| \tilde{\psi}(t_{k+i-1}) - \tilde{\psi}^k(t_{k+i-1}) \right\|_2 \\
& \quad + \frac{C_{\mathbf{f}} L}{2} \sum_{i=1}^l b_{k+i}^2 + \left\| \xi_{k+l} - \xi_k \right\|_2 \\
& \leq L \sum_{i=1}^l b_{k+i} \left\| \tilde{\psi}(t_{k+i-1}) - \tilde{\psi}^k(t_{k+i-1}) \right\|_2 \\
& \quad + \frac{C_{\mathbf{f}} L}{2} \sum_{i=1}^{k_T} b_{k+i}^2 + \sup_{1 \leq l \leq k_T} \left\| \xi_{k+l} - \xi_k \right\|_2.
\end{aligned} \tag{106}$$

Applying Lemma 6 to (106) and letting

$$C = \frac{C_{\mathbf{f}} L}{2} \sum_{i=1}^{k_T} b_{k+i}^2 + \sup_{1 \leq l \leq k_T} \left\| \xi_{k+l} - \xi_k \right\|_2,$$

yields

$$\begin{aligned}
& \sup_{t \in [t_k, t_{k+k_T}]} \left\| \tilde{\psi}(t) - \tilde{\psi}^k(t) \right\|_2 \\
& \leq C_e \left\{ \frac{C_{\mathbf{f}} L}{2} [c(k) - c(k + k_T)] \right. \\
& \quad \left. + \sup_{1 \leq l \leq k_T} \left\| \xi_{k+l} - \xi_k \right\|_2 \right\} + \frac{C_{\mathbf{f}} C_{k+1}}{2},
\end{aligned} \tag{107}$$

where $C_e \triangleq e^{L(T+b_1)}$, and $c(k) \triangleq \sum_{i>k} b_i^2$. Letting $k = \tilde{k}(l)$ in (107), we have $k + k_T = \tilde{k}(l+1)$ due to the definition of $T_{l+1} = t_{\tilde{k}(l+1)}$ in Step 2 of Appendix E and

$$\begin{aligned}
& \sup_{t \in I_l} \left\| \tilde{\psi}(t) - \tilde{\psi}^{\tilde{k}(l)}(t) \right\|_2 \\
& \leq C_e \left\{ \frac{C_{\mathbf{f}} L}{2} [c(\tilde{k}(l)) - c(\tilde{k}(l+1))] \right. \\
& \quad \left. + \sup_{\tilde{k}(l) \leq p \leq \tilde{k}(l+1)} \left\| \xi_p - \xi_{\tilde{k}(l)} \right\|_2 \right\} + \frac{C_{\mathbf{f}} b_{\tilde{k}(l)+1}}{2}.
\end{aligned} \tag{108}$$

Suppose that the step size $\{b_k : k > 0\}$ satisfies

$$C_e \frac{C_{\mathbf{f}} L}{2} [c(\tilde{k}(l)) - c(\tilde{k}(l+1))] + \frac{C_{\mathbf{f}} b_{\tilde{k}(l)+1}}{2} < \frac{\delta}{2}, \tag{109}$$

for $l \geq 0$.

Given $\sup_{t \in I_l} \left\| \bar{\mathbf{x}}(t) - \tilde{\mathbf{x}}^{\tilde{k}(l)}(t) \right\| > \delta$, we can obtain from (108) and (109) that

$$\begin{aligned}
& \sup_{\tilde{k}(l) \leq p \leq \tilde{k}(l+1)} \left\| \xi_p - \xi_{\tilde{k}(l)} \right\|_2 \\
& \geq \frac{1}{C_e} \left(\sup_{t \in I_l} \left\| \tilde{\psi}(t) - \tilde{\psi}^{\tilde{k}(l)}(t) \right\|_2 - \frac{C_{\mathbf{f}} L}{2} [c(\tilde{k}(l)) \right. \\
& \quad \left. - c(\tilde{k}(l+1))] - \frac{C_{\mathbf{f}} b_{\tilde{k}(l)+1}}{2} \right) \\
& > \frac{1}{C_e} \left(\sup_{t \in I_l} \left\| \bar{\mathbf{x}}(t) - \tilde{\mathbf{x}}^{\tilde{k}(l)}(t) \right\| - \frac{\delta}{2} \right) \\
& > \frac{\delta}{2C_e}.
\end{aligned}$$

Then, we get

$$\begin{aligned}
& P \left(\sup_{t \in I_m} \left\| \bar{\mathbf{x}}(t) - \tilde{\mathbf{x}}^{\tilde{k}(l)}(t) \right\| > \delta \right) \\
& \leq P \left(\sup_{\tilde{k}(l) \leq p \leq \tilde{k}(l+1)} \left\| \xi_p - \xi_{\tilde{k}(l)} \right\|_2 > \frac{\delta}{2C_e} \right) \\
& \leq P \left(\sup_{t \in I_i} \left\| \bar{\mathbf{x}}(t) - \tilde{\mathbf{x}}^{\tilde{k}(i)}(t) \right\| \leq \delta, 0 \leq i < l \right) \\
& \stackrel{(a)}{=} P \left(\sup_{\tilde{k}(l) \leq p \leq \tilde{k}(l+1)} \left\| \xi_p - \xi_{\tilde{k}(l)} \right\|_2 > \frac{\delta}{2C_e} \right),
\end{aligned} \tag{110}$$

where step (a) is due to the independence of noise, i.e., $\xi_p - \xi_{\tilde{k}(l)}, \tilde{k}(l) \leq p \leq \tilde{k}(l+1)$ are independent of $\hat{\mathbf{x}}_k, 0 \leq k \leq \tilde{k}(l)$.

The lower bound of the probability that the sequence $\{\hat{\mathbf{x}}_k : k \geq 0\}$ remains in the invariant set \mathcal{I} is given by

$$\begin{aligned}
& P(\hat{\mathbf{x}}_k \in \mathcal{I}, \forall k \geq 0) \\
& \stackrel{(a)}{\geq} P\left(\sup_{t \in I_m} \|\bar{\mathbf{x}}(t) - \tilde{\mathbf{x}}^{\tilde{k}(l)}(t)\| \leq \delta, \forall l \geq 0\right) \\
& \stackrel{(b)}{\geq} 1 - \sum_{l \geq 0} P\left(\sup_{t \in I_m} \|\bar{\mathbf{x}}(t) - \tilde{\mathbf{x}}^{\tilde{k}(l)}(t)\| > \delta\right) \\
& \stackrel{(c)}{\geq} 1 - \sum_{l \geq 0} P\left(\sup_{\tilde{k}(l) \leq p \leq \tilde{k}(l+1)} \|\xi_p - \xi_{\tilde{k}(l)}\|_2 > \frac{\delta}{2C_e}\right),
\end{aligned} \tag{111}$$

where step (a) is due to Lemma 4, step (b) is due to Lemma 4.2 in [26], and step (c) is due to (110). Let $\|\cdot\|_\infty$ denote the max-norm, i.e., $\|\mathbf{u}\|_\infty = \max_l |\mathbf{u}_l|$. Note that for $\mathbf{u} \in \mathbb{R}^D$, $\|\mathbf{u}\|_2 \leq \sqrt{D} \|\mathbf{u}\|_\infty$. Hence we have

$$\begin{aligned}
& P\left(\sup_{\tilde{k}(l) \leq p \leq \tilde{k}(l+1)} \|\xi_p - \xi_{\tilde{k}(l)}\|_2 > \frac{\delta}{2C_e}\right) \\
& \leq P\left(\sup_{\tilde{k}(l) \leq p \leq \tilde{k}(l+1)} \|\xi_p - \xi_{\tilde{k}(l)}\|_\infty > \frac{\delta}{4C_e}\right) \\
& = P\left(\sup_{\tilde{k}(l) \leq p \leq \tilde{k}(l+1)} \max_{1 \leq s \leq 4} |[\xi_p]_s - [\xi_{\tilde{k}(l)}]_s| > \frac{\delta}{4C_e}\right) \\
& = P\left(\max_{1 \leq s \leq 4} \sup_{\tilde{k}(l) \leq p \leq \tilde{k}(l+1)} |[\xi_p]_s - [\xi_{\tilde{k}(l)}]_s| > \frac{\delta}{4C_e}\right) \\
& \leq \sum_{s=1}^4 P\left(\sup_{\tilde{k}(l) \leq p \leq \tilde{k}(l+1)} |[\xi_p]_s - [\xi_{\tilde{k}(l)}]_s| > \frac{\delta}{4C_e}\right).
\end{aligned} \tag{112}$$

With the increasing σ -fields $\{\mathcal{G}_k : k \geq 0\}$ defined in Appendix D, we have for $k \geq 0$,

- 1) $\xi_k = \sum_{l=1}^k b_l \hat{\mathbf{z}}_l \sim \mathcal{N}(0, \sum_{l=1}^k a_k^2 \mathbf{I}(\hat{\psi}_{l-1}, \mathbf{W}_l)^{-1})$,
- 2) ξ_k is \mathcal{G}_k -measurable, i.e., $\mathbb{E}[\xi_k | \mathcal{G}_k] = \xi_k$,
- 3) $\mathbb{E}[\|\xi_k\|_2^2] = \sum_{l=1}^k b_l^2 \text{tr}(\mathbf{I}(\hat{\psi}_{l-1}, \mathbf{W}_l)^{-1}) < \infty$,
- 4) $\mathbb{E}[\xi_k | \mathcal{G}_l] = \xi_l$ for all $0 \leq l < k$.

Therefore, $[\xi_k]_s, s = 1, 2, 3, 4$ is a Gaussian martingale with respect to \mathcal{G}_k , and satisfies

$$\begin{aligned}
\text{Var}[[\xi_{k+l}]_s - [\xi_k]_s] &= \sum_{i=k+1}^{k+l} b_i^2 [\mathbf{I}(\hat{\psi}_{i-1}, \mathbf{W}_i)^{-1}]_{s,s} \\
&\leq \sum_{i=k+1}^{k+l} b_i^2 \frac{C_{\mathbf{I}} \sigma^2}{|s_p|^2} \\
&= \frac{C_{\mathbf{I}} \sigma^2}{|s_p|^2} [c(k) - c(k+l)],
\end{aligned} \tag{113}$$

where $C_{\mathbf{I}} \triangleq \max_s \max_{i \geq 1} \frac{|s_p|^2}{\sigma^2} [\mathbf{I}(\hat{\psi}_{i-1}, \mathbf{W}_i)^{-1}]_{s,s}$. Let $\eta = \frac{\delta}{4C_e}$, $M_i = [\xi_{\tilde{k}(l)+i}]_s - [\xi_{\tilde{k}(l)}]_s, s = 1, 2, 3, 4$ and $p =$

$\tilde{k}(l+1) - \tilde{k}(l)$ in Lemma 7, then from (112) and (113), we can obtain

$$\begin{aligned}
& P\left(\sup_{\tilde{k}(l) \leq p \leq \tilde{k}(l+1)} |[\xi_p]_s - [\xi_{\tilde{k}(l)}]_s| > \frac{\delta}{4C_e}\right) \\
& \leq 2 \exp\left\{-\frac{\delta^2}{32C_e^2 \text{Var}[[\xi_{\tilde{k}(l)+i}]_s - [\xi_{\tilde{k}(l)}]_s]}\right\} \\
& \leq 2 \exp\left\{-\frac{\delta^2 |s_p|^2}{32C_{\mathbf{I}} C_e^2 [c(\tilde{k}(l)) - c(\tilde{k}(l+1))]\sigma^2}\right\}.
\end{aligned} \tag{114}$$

Combining (111), (112) and (114), we have

$$\begin{aligned}
& P(\hat{\mathbf{x}}_k \in \mathcal{I}, \forall k \geq 0) \\
& \geq 1 - 6 \sum_{l \geq 0} \exp\left\{-\frac{\delta^2 |s_p|^2}{32C_{\mathbf{I}} C_e^2 [c(\tilde{k}(l)) - c(\tilde{k}(l+1))]\sigma^2}\right\}.
\end{aligned} \tag{115}$$

To use Lemma 8, we assume that the step-size b_k satisfies

$$c(0) = \sum_{i>0} b_i^2 \leq \frac{\delta^2 |s_p|^2}{32C_{\mathbf{I}} C_e^2 \sigma^2}. \tag{116}$$

Then, from Lemma 8, we can obtain

$$\begin{aligned}
& \frac{\exp\left\{-\frac{\delta^2 |s_p|^2}{32C_{\mathbf{I}} C_e^2 [c(\tilde{k}(l)) - c(\tilde{k}(l+1))]\sigma^2}\right\}}{c(\tilde{k}(l)) - c(\tilde{k}(l+1))} \\
& \leq \frac{\exp\left\{-\frac{\delta^2 |s_p|^2}{32C_{\mathbf{I}} C_e^2 c(0)\sigma^2}\right\}}{c(0)},
\end{aligned}$$

for $c(\tilde{k}(l)) - c(\tilde{k}(l+1)) < c(\tilde{k}(l)) \leq c(0)$. Hence, we have

$$\begin{aligned}
& \sum_{l \geq 0} \exp\left\{-\frac{\delta^2 |s_p|^2}{32C_{\mathbf{I}} C_e^2 [c(\tilde{k}(l)) - c(\tilde{k}(l+1))]\sigma^2}\right\} \\
& \leq \sum_{l \geq 0} [c(\tilde{k}(l)) - c(\tilde{k}(l+1))] \cdot \frac{\exp\left\{-\frac{\delta^2 |s_p|^2}{32C_{\mathbf{I}} C_e^2 c(0)\sigma^2}\right\}}{c(0)} \\
& = c(0) \cdot \frac{\exp\left\{-\frac{\delta^2 |s_p|^2}{32C_{\mathbf{I}} C_e^2 c(0)\sigma^2}\right\}}{c(0)} = \exp\left\{-\frac{\delta^2 |s_p|^2}{32C_{\mathbf{I}} C_e^2 c(0)\sigma^2}\right\}.
\end{aligned} \tag{117}$$

As $C_e = e^{L(T+b_1)}$, $c(0) = \sum_{i>0} b_i^2$, and b_k, T, L are given by (18), (83), (103) separately, we can obtain

$$\begin{aligned}
\frac{\delta^2 |s_p|^2}{32C_{\mathbf{I}} C_e^2 c(0)\sigma^2} &= \frac{\delta^2 |s_p|^2}{32C_{\mathbf{I}} e^{2L(T+\frac{\alpha}{K_0+1})} \sigma^2 \sum_{i \geq 1} \frac{\epsilon^2}{(i+K_0)^2}} \\
&= \frac{\delta^2}{\sum_{i \geq 1} \frac{32C_{\mathbf{I}} e^{2L(T+\frac{\epsilon}{K_0+1})}}{(i+K_0)^2}} \cdot \frac{|s_p|^2}{\epsilon^2 \sigma^2}.
\end{aligned} \tag{118}$$

In (118), $0 < \delta < \inf_{\mathbf{v} \in \partial \mathcal{B}} \|\mathbf{v} - \hat{\mathbf{x}}_b\|$, (109) and (116) should be satisfied, where a sufficiently large $K_0 \geq 0$ can make both (109) and (116) true.

To ensure that $\hat{\mathbf{x}}_0 + b_1 \left[\mathbf{f} \left(\hat{\Psi}_0, \Psi \right) \right]_{3,4}$ does not exceed the mainlobe $\mathcal{B}(\mathbf{x})$, i.e., the first step-size b_1 satisfies

$$\begin{aligned} \left| \hat{x}_{0,1} + b_1 \left[\mathbf{f} \left(\hat{\Psi}_0, \Psi \right) \right]_3 - x_1 \right| &< 1 \\ \left| \hat{x}_{0,2} + b_1 \left[\mathbf{f} \left(\hat{\Psi}_0, \Psi \right) \right]_4 - x_2 \right| &< 1 \end{aligned}$$

we can obtain the maximum ϵ as follows

$$\epsilon_{\max} = \min \frac{(K_0 + 1)(1 - |x_1 - \hat{x}_{0,1}|)}{\left| \left[\mathbf{f} \left(\hat{\Psi}_0, \Psi \right) \right]_3 \right|}, \frac{(K_0 + 1)(1 - |x_2 - \hat{x}_{0,2}|)}{\left| \left[\mathbf{f} \left(\hat{\Psi}_0, \Psi \right) \right]_4 \right|}.$$

Hence, from (118), we have

$$\frac{\delta^2 |s_P|^2}{32C_1 C_e^2 c(0) \sigma^2} \cdot \frac{\epsilon^2 \sigma^2}{|s_p|^2} \geq \frac{\delta^2}{\sum_{i \geq 1} \frac{32C_1 e^{2L(T + \frac{\epsilon_{\max}}{K_0 + 1})}}{(i + K_0)^2}} \triangleq C. \quad (119)$$

Combining (115), (117) and (119), yields

$$P(\hat{\mathbf{x}}_k \in \mathcal{I}, \forall k \geq 0) \geq 1 - 8e^{-\frac{C|s_p|^2}{\epsilon^2 \sigma^2}},$$

which completes the proof.